LEAST ACTION PRINCIPLE FOR REAL-TIME MITIGATION OF ANGLE INSTABILITY IN POWER SYSTEMS

By

MICHAEL SHERWOOD

A thesis submitted in partial fulfillment of

the requirements for the degree of

MASTER OF SCIENCE IN ELECTRICAL ENGINEERING

WASHINGTON STATE UNIVERSITY

School of Elecrtical Engineering and Computer Science

DECEMBER 2007

To the Faculty of Washington State University:

The members of the Committee appointed to examine the thesis of MICHAEL SHERWOOD find it satisfactory and recommend that it be accepted.

_____
Chair

_____

_____

ACKNOWLEDGMENT

For his patience and guidance in the work presented in this dissertation I sincerely thank my advisor Vaithianathan Venkatasubramanian. His knowledge and experience in power systems has been a great asset in developing my understanding of the advanced topics researched in this thesis. I would also like to thank him and the school of EECS for financially supporting me while working towards my M.S.

LEAST ACTION PRINCIPLE FOR REAL-TIME MITIGATION OF ANGLE INSTABILITY IN POWER SYSTEMS

ABSTRACT

By Michael Sherwood, M.S.
Washington State University
December 2007

Chair: Vaithianathan Venkatasubramanian

The use of synchrophasors in power systems has been increasing due to the necessity in real-time monitoring of critical areas in a system. The advantages of synchrophasors are evident in their use in the Wide Area Monitoring System where monitoring the voltage magnitudes and angles in real-time is critical in maintaining operational reliability. Problems arising from deregulation combined with excessive loading have made power systems less secure. To help alleviate these issues, it is essential that the reliability status of a system can be assessed as quickly as possible. Synchrophasors combined with a high speed communication network can allow development of automatic control actions, which in turn give operators more time to take preventive actions to keep the system from collapsing.

The use of synchrophasors or Phasor Measurement Units in automatic generation shedding schemes, as well as load shedding schemes have been proposed in the past. When such an action is initiated, it is extremely important to know that it is the correct one to take since load shedding results in customer inconvenience and lost revenue. On the other hand the total loss of a system such as from blackouts leads to an adverse impact on society. One method for determining the stability is the transient energy function. The use of transient energy functions in determining stability has shown potential in determining load or generation shedding. The computation of transient energy functions using real-time data from synchrophasors is therefore an attractive solution to mitigating stability.

Least action principle is proposed in theoretical physics for abstract modeling. Here, the concepts of least action principle are applied for assessing and mitigating angle instability in power systems. From the computation of potential and kinetic energy, a different quantity known as the Lagrangian is formed. The Effort, which is the time integral of the Lagrangian, is then calculated and is used in determining the critical generators for initiating generation shedding. The IEEE New England 39 bus test system is used to test the algorithms. From the results it appears that the use of Effort of each machine is reliable in determining the set of critical generators following a disturbance.

TABLE OF CONTENTS

ACKNOWLEDGMENT iii
ABSTRACT iv
TABLE OF CONTENTS vi
LIST OF TABLES vii
LIST OF FIGURES viii
LIST OF FIGURES viii
CHAPTER 1 INTRODUCTION 1
1.1 Overview 1
1.2 Load Shedding 6
CHAPTER 2 TRANSIENT ENERGY FUNCTIONS 8
2.1 Introduction 8
2.2 Formulation 8
2.3 Lyapunov's Second Theorem 11
2.4 Implementation 12
2.5 Conclusions 16
CHAPTER 3 LAGRANGIAN AND EFFORT 17
3.1 Introduction 17
3.2 Formulation 17
3.3 Implementation 20
3.4 Determining Stability Limits 24
3.5 Conclusions 25
CHAPTER 4 ANGLE MITIGATION ALGORITHM 27
4.1 Introduction 27
4.2 Formulation 28
4.3 Implementation 28
4.4 Conclusions 29
CHAPTER 5 RESULTS AND COMPARISONS 31
5.1 New England 39 Bus Test System Fault Case 31
5.1.1 New England 39 Bus Test System Overloaded Case 33
5.2 39 Bus 3 Area System Fault Case 39
5.2.1 39 Bus 3 Area System Heavy Loading Case 49
5.3 Communication Delay Effect 56
CHAPTER 6 CONCLUSIONS 59
CHAPTER 7 REFERENCES 61
CHAPTER 8 APPENDIX 63

LIST OF TABLES

Table 3- 1: Load to Generation Ratio, 39 Bus 3-Area System 21
Table 3- 2: Control Times Comparisons For Fault At Bus 4 24

Table 5- 1: Unmodified 39 Bus System Thresholds 31
Table 5- 2: Control Times For Unmodified 39 Bus System 32
Table 5- 3: Critical Clearing Time Increase Using Effort Control Times 33
Table 5- 4: Unstable Cont 1 Algorithm Comparisons 37
Table 5- 5: High Loading Level Comparisons 37
Table 5- 6: Max Loading Thresholds 39
Table 5- 7: Thesholds For 20% Less Load 39
Table 5- 8: Thresholds For 40% Less Load 40
Table 5- 9: Unstable Cases Using Maximum Loading 40
Table 5- 10: Unstable Cases Using 20% Less Load Of Maximum 42
Table 5- 11: Unstable Cases With 40% Less Load From Maximum 44
Table 5- 12: CCT With/ Without Control Action Max Loading 46
Table 5- 13: CCT With/Without Control Action, -20% Load 47
Table 5- 14: CCT With/Without Control Action, -40% Load 48
Table 5- 15: Excessive Loading, 3-Area System 49
Table 5- 16: Recommended Voltage Protection Delay Times 55
Table 5- 17: Frequency Relay Delay Times 56
Table 5- 18: Time Delay, Effort Algorithm 57
Table 5- 19: Time Delay, Lagrangian Algorithm 57
Table 5- 20: Time Delay, Angle Algorithm 58
Table 5- 21: Time Delay, Energy Algorithm 58

Table A- 1: 39 Bus Overload Contingencies 65
Table A- 2: Exciter Parameters 65
Table A- 3: 39 Bus Governor Parameters 66
Table A- 4: Generator 1 to 9 Parameters 66
Table A- 5: Generator 10 Classical Model Parameters 66

LIST OF FIGURES

Figure 2- 1: TE Threshold Gen4..... 13
Figure 2- 2: Kinetic Energy Gen 4..... 14
Figure 2- 3: Potential Energy Gen4..... 15
Figure 2- 4: Gen 4 Total Energy, Fault Bus 29 15

Figure 3- 1: System Lagrangian, Unstable Fault Case 18
Figure 3- 2: Computation of Lagrange for each generator, no fault simulated 19
Figure 3- 3: Sum of Lagrangians for Cont1, Stable 19
Figure 3- 4: Estimated Rotor Angle from Bus Voltage Angle Measurement 21
Figure 3- 5: Effort Computed for method 1 22
Figure 3- 6: Effort Using Method 2 23
Figure 3- 7: Effort Comparison Between Methods 23
Figure 3- 8: Gen 3 Lagrangian Stability Limit 24
Figure 3- 9: Gen 3 Stability Limit Using Effort 25

Figure 4- 1: Estimated Rotor Angle From Voltage Angle..... 29

Figure 5- 1: Rotor Angle Estimated From Bus Voltage Angle 34
Figure 5- 2: Total System Lagrangian for Unstable Cont2..... 35
Figure 5- 3: Effort for Unstable Cont2 35
Figure 5- 4: Lagrange Computation for Unstable Cont1..... 36
Figure 5- 5 Energy for Unstable Cont1..... 36
Figure 5- 6: Lagrangian for Stable Cont 4 38
Figure 5- 7: Rotor Angle For 3-Area Over Load Case..... 50
Figure 5- 8: Lagrangian Computation for Unstable Cont4 51
Figure 5- 9: Energy Computation for Unstable Cont4..... 51
Figure 5- 10: Effort Computation Unstable Cont4..... 52
Figure 5- 11: Load Shedding For Contingency 2..... 53
Figure 5- 12: Unstable Cont. 2 Rotor Angle..... 54
Figure 5- 13: Unstable Cont. 2 Rotor Frequency..... 54
Figure 5- 14: Voltage Magnitude, Unstable Cont 2 55

Figure A- 1: 39 Bus 3 Area Test Case 63
Figure A- 2: Original New England 39 Bus System..... 64

CHAPTER 1 INTRODUCTION

1.1 OVERVIEW

Operational reliability of large power systems has received much attention in the past decade because of deregulation and ever increasing loads. One of the more recent events was the August 2003 blackout which occurred in the North Eastern United States, it was estimated to have cost roughly 6 billion USD in lost revenue alone, apart from the societal impact [3]. In determining corrective actions to prevent such events from occurring, it was found that providing better real-time tools for operators was a top priority [4]. The emergence of synchrophasors in monitoring power system conditions seems to be an attractive solution for monitoring real-time operational reliability status. Knowing the voltages at each bus in real-time is only part of the solution. From the point of view of angle stability, we also need to know whether or not a generator or group of generators will become unstable based on interactions with other components in the system.

In transient stability of power systems, it is critical that the operating frequency and voltage levels stay within an adequate level. Voltage stability is relatively slower phenomenon since we typically know that the areas with the lowest voltage levels and reactive power reserves are the critical areas where corrective actions will have the greatest impact on mitigating voltage stability. Angle stability on the other hand is not as easy to analyze. Although it is defined as the ability for the generators in a system to remain in synchronism, it is a much faster phenomenon and is not as clearly understood. In some cases, a system may not go angle unstable on the first swing. In such a case it is

not as apparent which modes or mechanisms are causing the system to lose synchronism. Whether or not the system is heavily loaded at the time of disturbance is also important since under such stressed conditions the swings can not be easily distinguished as being stable or unstable right away [5]. When this happens, generators that may initially appear stable will later follow the other unstable generators rather then staying in synchronism with the rest of the system. Being able to prevent such an event is beneficial in maintaining stability.

Looking again at the August 2003 blackout we see that eventual loss of generators and transmission lines rapidly lead to the loss of synchronism between different areas [3]. From the data given in the August 14th blackout report we see that the loss of synchronism happens in the order of seconds whereas the voltage declines that preceded took minutes. An approach that seems well suited for real-time stability assessment is the transient energy function and the angle algorithm proposed earlier by Dongchen Hu [7].

The use of transient energy functions is one method used for determining stability. With recent advances in data acquisition using synchrophasors, the estimation of frequency and rotor angle can be accomplished in less then a second. This is a significant time reduction when comparing with traditional state estimation that takes minutes to complete. To see how synchrophasors apply to transient energy functions a brief description of how they are computed is in order.

Transient energy functions are computed by using the kinetic energy and potential energy of a machine. In previous attempts to use the energy function the energy dissipated in the transmission network was estimated [1]. In the use of transient energy functions applied in this dissertation it is assumed that this dissipated energy is negligible.

What we then have is the kinetic energy as a function of rotor frequencies and the potential energy as a function of rotor angle displacements. The summation of these two terms for each machine gives the total energy of that machine. Since the total energy is a function of quantities easily measured by synchrophasors it is obvious that the total energy can be computed almost as quickly as the data becomes available. By studying the total energy of each machine we can see how much energy each machine can produce or absorb from the system before losing synchronism with the grid.

Several new approaches to using the individual energy functions are proposed. The Lagrangian, which is based upon the difference rather then the sum of the kinetic and potential energy, can be used in determining dynamic stability in the same way as the total energy. There are several advantages to using the Lagrangian over the total energy which will be discussed in the later chapters. The physical meaning of the Lagrangian is somewhat vague since it is used in Classical Physics as a modeling principle to determine the equations of motion of a system. Conceptually we can visualize the Lagrangian as an indication in which way the energy is being converted between the kinetic and potential energy. The Lagrangian is treated in the same way as the total energy by noticing that a maximum amount can be obtained by each machine before instability occurs. The Lagrangian is shown in this thesis to indicate instability faster then by using the total energy.

A new approach in detecting instability is the use of Effort for the individual machines. In classical physics, Effort is known as the Action. Effort, or Action, is given by the integral of the Lagrangian over time. Interestingly enough, the minimum of the action, known as the principle of least action, gives us to determine a set of equations

which describe the motion of the system. Newton's laws of motion are the more commonly used alternate method fore deriving the dynamic equations. In this Thesis, Least Action Principle is applied in the context of real-time stability.

Since the Lagrangian is being computed in real-time, it makes computing the Effort a straightforward procedure. To find the limiting amount of Effort that a generator can assert, we integrate the Lagrangian along the trajectories corresponding to the fault scenario, with duration equal to the critical clearing time, near the given generator. For disturbances dealing with only faults, we calculate the Effort for the fault duration, and if the Effort exceeds the maximum amount needed for maintaining stability we take preventive action to maintain synchronism. Since it is difficult to know that there is a fault until it has been detected and cleared, we will also look at cases where the sum of the Lagrangians over all machines is used as a trigger to start computation of the Effort.

By looking at the rotor angle alone we can also determine generators that are losing synchronism with the system. This method was proposed recently in [19] and by Dongchen Hu [7]. The algorithm works by taking the estimated rotor angle and comparing with a set threshold. Once the threshold is exceeded the rotor angle is integrated and if the integral exceeds a set amount before the rotor angle begins decreasing then control action is taken. The advantage of this is it takes away from the over sensitivity of only looking at the rotor angle, which can change depending on the modes of instability. The results of Dongchen's algorithm, which will be called the angle algorithm from this point on, are compared with the transient energy function, Lagrangian and Effort to determine accuracy between algorithms.

The terms rotor angle and rotor frequency used in this dissertation represent the aproximate rotor angle and frequency. This refers to the synchrophasors measurements taken at the generator terminal bus. The bus voltage angle is approximately equivalent to the rotor angle with regards to its use in the preceding work. This assumption is made based on the premise that the bus is located electrically near the generator, in other words the only impedance between the bus and the internal voltage is the synchronous reactance. From simulations on the 39 bus a difference ranging from 1 to 20 degrees was observed but this is an irrelevant difference since we are referring the bus voltage angle on a center of inertia frame, not to mention that the critical energy is calculated using the bus voltage angle. The frequency on the other hand is not measured directly. It is computed from the bus voltage angle and noting the change in angle with respect to time. This can be accomplished easily since each data point has a time stamp associated with it.

The structure of this dissertation is as follows. In Chapter 2, we discuss the transient energy function that has been proposed with only the individual machine energy being computed. The model is modified to be used with synchrophasors data referenced on a system wide center of inertia frame of reference. The use of center of inertia is implemented on both rotor angle and frequency estimates. In Chapter 3, the Lagrangian and Effort are introduced. Since the computation of Effort follows from the Lagrangian it seems fitting to include them both in the same chapter. The angle algorithm is introduced in Chapter 4 with its formulation given in [7]. In Chapter 5 the algorithms are tested on two variations of the 39 bus system. In the first setup, we treat each generator as a separate area making the plant modes more prevalent then the inter-area modes. The loading was varied to make the system more or less stressed. For the second setup

several transmission lines are removed from the system and the impedances of the tie-lines between areas are increased (i.e. the line length increased) in order to test the algorithms more thoroughly. The severity of the loading in the system is then varied to determine the accuracy of each algorithm with regards to different thresholds, taken at light, medium and heavy loading.

A few remarks regarding the dynamic data used in the simulations should be stated. First off the original dynamic data included power system stabilizers. These have been removed from the models. Governor models have been added on all generators except for Generator 10 located at bus 39. The droops on each generator governors vary from 15% to 30%. The classical model was used for Generator 10 and the two axis model for the rest of the generators.

1.2 LOAD SHEDDING

From conducting simulations the proposed algorithms discussed so far have been shown to be well suited for determining generation shedding. Load shedding has been difficult to determine just from using these algorithms. From the 39 bus 3 area test system, we can see that area 2 is significantly more loaded then the other two areas. As a consequence we see that area two is importing a significant amount of power from the other two areas. We would then expect that shedding load in area 2 would have a greater effect on mitigating angle instability then for shedding load in the other two areas. Looking at the center of inertia for with respect to rotor angle and frequency we cannot tell at the time when control action is taken if load shedding should occur. This is because if a fault occurs in the heavily loaded area then the machines will accelerate for a short time while the transmission line is still faulted. Although in the long term we would

see the frequency to decay in this area, we can not predict it for certain by using the proposed algorithms. In the following simulations, a simple algorithm is proposed to determine the most suitable area for load shedding.

This indexing for each area is based on the load to generation ratio for that area. More specifically we take the total load in the area and divide by the total generation of the system, shown in equation 1-1.

$$R_{L/G}^{i} = \frac{Load_i}{\sum_{i=1}^{k} Gen_i} \qquad (1.1)$$

Equation 1.1 is evaluated at the time of control action and the area with the highest ratio is the candidate area for load shedding. For simplicity, we shed the same amount of load as generation.

CHAPTER 2 TRANSIENT ENERGY FUNCTIONS

2.1 INTRODUCTION

The use of transient energy functions in determining stability has shown promise as seen from previous research [1]. Transient energy functions are a means of estimating the energy in a system. Knowing the energy allows us to understand the behavior of a system without having to run time-domain simulations to determine if the trajectories are stable. Since the trajectories, rotor angle and frequency, are referenced on a center of inertia then the energy is also referenced the same. This makes identifying the critical generators significantly easier since we can directly see if they are accelerating or decelerating away from the rest of the system. We will further assume that the energy of each generator is initially zero for the start of each simulation. This has been shown to be a reasonable assumption in previous work [1][5]. Simulations on the 39 bus system have also shown that the energy changes insignificantly from load changes compared to the energy from sustained faults making any small deviations from the initial energy from zero irrelevant.

2.2 FORMULATION

To start off the definition of center of inertia is re-stated here. The definition of center of angle using the generator inertia H is given by the following,

$$\delta_{COA} = \frac{\sum_{i=1}^{N} \bar{\delta}_i H_i}{\sum_{i=1}^{N} H_i}$$

In theory the inertia H is computed for each generator and is therefore ready to use for real-time computation. However the generator at a given bus might represent an equivalent group of many generators, in this case making the exact calculation of H for that equivalent generator difficult to compute. A scenario that makes using H difficult is where generators within a plant are committed or de-committed as load changes through out the day. A new approach using the scheduled power output is used as a weighting in the center of angle was proposed in [19]. The new center of inertia is given in equation 2.1,

$$\delta_{COA}^{k} = \frac{\sum_{i=1}^{N} \bar{\delta}_i P_{T_i}}{\sum_{i=1}^{N} P_{T_i}} \qquad (2.1)$$

In 2.1 δ_i is the bus voltage angle estimate of the rotor angle for the ith generator in area k. For a system represented as one single area, the center of inertia is computed using all the generators online. Once the center of inertia is computed, we then reference the rotor angles to it as shown in 2.2.

$$\theta_i^k = \delta_i^k - \delta_{COA}^k \qquad (2.2)$$

The rotor frequency is computed on the center of inertia frame of reference in the same way. This is shown in 2.3 and 2.4,

$$\omega_{COA}^{k} = \frac{\sum_{i=1}^{N} \bar{\omega}_i P_{T_i}}{\sum_{i=1}^{N} P_{T_i}} \qquad (2.3)$$

$$\tilde{\omega}_i^k = \dot{\delta}_i^k - \dot{\delta}_{COA}^k \qquad (2.4)$$

To understand the transient energy function better, let us look at the swing equations of the synchronous generator defined on the center of inertia given in [1],

$$\mathrm{M}_i\dot{\tilde{\omega}}_i = P_{mi} - P_{ei} - D_i\tilde{\omega}_i \qquad (2.5)$$

Equation 2.5 tells us the acceleration, or deceleration, due to the mismatch between mechanical power P_{mi} on the shaft and the electrical power P_{ei} which opposes it. The damping D_i is assumed to have a negligible effect on the first swing and therefore is set to zero. Another term appearing on the right hand side of 2.5, $-P_{COA}^{k}$ is used in [1][5] which relates the power mismatch to the center of inertia power mismatch, however the swing equations used in this research will neglect this.

To relate the swing equation 2.5 to energy it is necessary to describe the fundamental relation between work, energy and power. Knowing the force acting on a body tells us the acceleration of that body by Newton's equation $F = m * a$. The torque that causes a body to rotate is proportional to the force by the distance from the center of mass. Noting that the swing equation essentially tells us the net torque on the generator shaft we can then state that it is proportional to a net force. Taking the first integral of motion of the swing equation then gives us work. Work is merely the change in kinetic energy of the system, and since energy is conserved this is also equal to the change in potential energy.

The mathematical derivation given in [5] is similar but instead of multiplying 2.5 by δ to get Work, i.e. $W = \tau * \theta$, we use the time derivative of delta $\dot{\delta}$ giving us power instead of work. This is done to make the integration easier. Integrating with respect to time gives us the work, which is equivalent to energy. Deriving the energy in this fashion makes integration easier since we know that $\dot{\delta}$ is equivalent to ω. Integrating 2.5,

$$\int \left(\mathrm{M}_i \dot{\tilde{\omega}} - P_{mi} + P_{ei} \right) \dot{\delta} * dt = \int \mathrm{M}_i \frac{d\omega}{dt} \omega * dt - \int \left(P_{mi} - P_{ei} \right) \frac{d\delta}{dt} * dt$$

Looking at the first integral term on the right hand side, we see that this is merely the chain rule used in differentiation so integrating this gives us $\frac{1}{2}\mathrm{M}_i \tilde{\omega}^2$. For the second term we see that *dt* cancels out so we are left with the integration with respect to angular displacement δ. At this point it, should be mentioned that Equation 2.5 was arranged such that $0 = \mathrm{M}_i \dot{\tilde{\omega}} - (P_{mi} - P_{ei})$. Integrating the term (zero) gives us a constant representing the total energy of the system which satisfies the theory of energy conservation. The transient energy function representing a single machine is given by equation 2.6,

$$TE_i = \frac{1}{2}\mathrm{M}_i \tilde{\omega}_i^2 - \int_{\delta_s}^{\delta} (P_{mi} - P_{ei}) d\delta \qquad (2.6)$$

2.3 LYAPUNOV'S SECOND THEOREM

The premise that transient energy functions are suitable for determining stability of a system is based on Lyapunov's Theorems of stability. In particular interest is Lyapunov's second method. The second method is based on finding an equation that tells us the behavior of the trajectories without explicitly integrating the differential equations which is computationally tedious. From the point of angle stability this means that the Lyapunov equation gives sufficient conditions on when the rotor angle and rotor frequency trajectories are asymptotically stable in the sense that they return to a stable equilibrium point. The Lyapunov function will be denoted as $V(x)$ in keeping with the traditional notation. For a function to be considered as a Lyapunov function it must be shown that the following characteristics apply [2],

1. $V(x)$ and its first derivative with respect to time, $\dot{V}(x)$, are continuous within a bounded region Ω.
2. $V(0) = 0$, $\dot{V}(x) < 0$ (negative definite
3. $V(x)$ is positive and bounded within a region Ω surrounding the origin.

It has been shown in [1], [5], that the transient energy function satisfies these conditions making it a suitable Lyapunov function. The third criterion has been shown to be true through simulation results as stated in [5]. The second criterion is easily verified by inserting the equilibrium points $\omega_i = \omega_s$ and $\delta_i = \delta_s$ into 2.6. The main problem is verifying the first criterion, that the estimated rotor angle and frequency are continuous. Any type of network changes will cause discontinuities in bus voltage angles and magnitudes. For instance a line tripping can show a difference especially if it is a main tie-line. Faults close to any generator will lead to an even larger discontinuity. As a solution to this problem a low pass filter is used on the synchrophasor's output.

2.4 IMPLEMENTATION

The online implementation of the transient energy function is assumed to be done through SCADA (Supervisory Control and Data Acquisition). SCADA gives the control operators a way to monitoring the power flows and voltage levels in a system. Traditionally this was done with state estimators but for convenience we will assume that the synchrophasor's measurements monitoring the output of each generator are used instead. This is a reasonable assumption since the generator output is metered anyways.

When implementing the transient energy function we compare the computed energy with the known critical amount of energy. If the maximum energy for a given

disturbance is less then the critical energy required for the machine to lose synchronism then it is stable. If the machine goes above this limit then it is unstable. For the case where a group of machines beginning to lose synchronism we take the machine that takes the shortest amount of time to go beyond its critical energy limit as the candidate machine where generation shedding should occur.

The critical energy is found through simulating a sustained fault with duration equal to the critical clearing time near the generator of interest. The following example shows the calculation of the critical energy for Generator 4 on the 39-bus 3 Area power system under heavy loading conditions. The maximum total energy for the generator is shown in Figure 2-1,

Figure 2- 1: TE Threshold Gen4

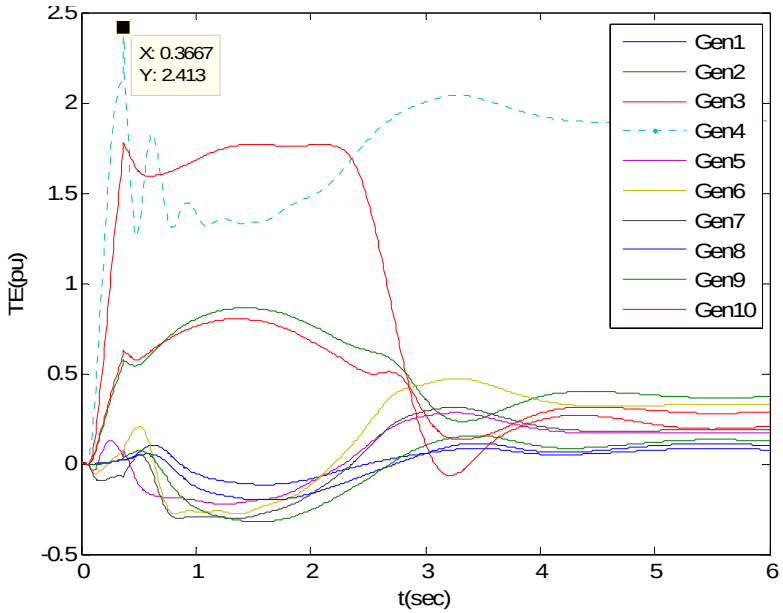

The total energy of Generator 4 is depicted in Figure 2-1 as the dotted line. The maximum total energy that is reached is 2.41pu. Looking at Figure 2-1 we see that the total energy does not go to zero. The reason for this is that we are integrating from the pre-fault equilibrium point, not the post-fault equilibrium point. To know the post fault

equilibrium point, we would need to do transient simulations for all possible faults, which is impractical for any reasonably sized system. We can see that the total energy remains bounded so it is considered stable even though the second Lyapunov condition is not entirely met. Examining the kinetic energy, we see that it does go to zero as shown in Figure 2-2,

Figure 2- 2: Kinetic Energy Gen 4

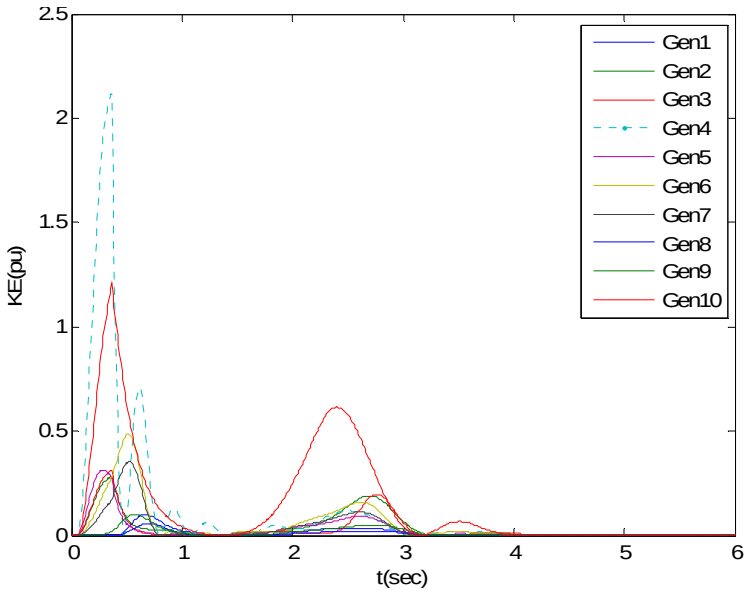

When all of the kinetic energy is converted to potential energy, we can say that the system is stable. This can be misleading since in power systems we consider a generator to be unstable when pole slipping occurs. Pole slipping is a phenomenon that we wish to avoid since it causes damage to the synchronous machine and other equipment. In reality there are protection schemes to prevent the machine from pole-slipping, so assuming the machine will trip we need to determine at what point we need to shed generation to prevent the generator from going offline completely.

In Figure 2-3 it is evident that the potential energy stops increasing as the kinetic energy is converted into potential energy.

Figure 2- 3: Potential Energy Gen4

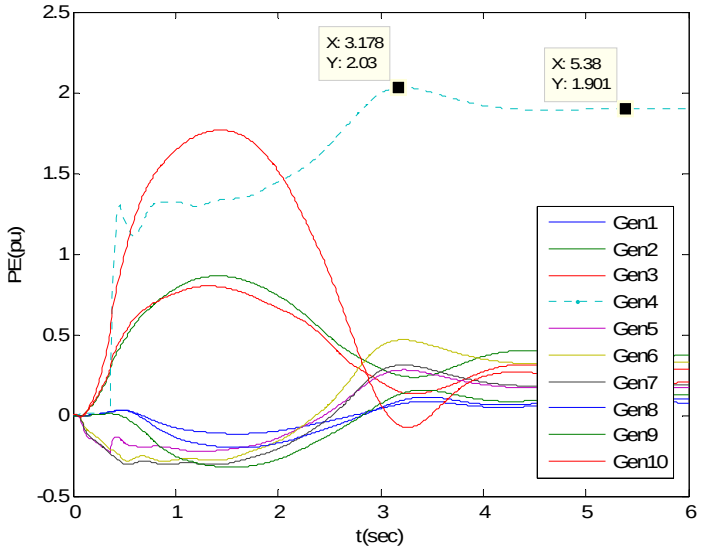

Let us look at the case where Generator 4 remains in synchronism with the system but other generators do not. In Figure 2-4, we observe that the total energy of Generator 4 does not exceed 2 pu, or come close to it.

Figure 2- 4: Gen 4 Total Energy, Fault Bus 29

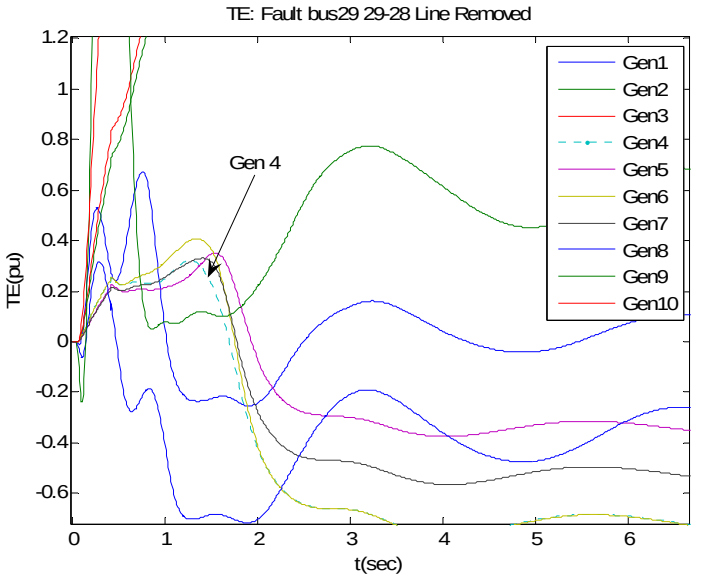

Generators 2, 3, and 10 diverge from the rest of the system where Generator 4 remains in synchronism. Another point that should be made is that the total energy of Generator 4 settles down to a value less than zero where as the unstable generators do not. In this

case, the unstable generators, those located in Area 2 in Figure A-1, decelerate since the Generation in Area 2 is not sufficient to supply the entire load in that area.

2.5 CONCLUSIONS

Determining the stability of a power system using total energy has its limitations. The most notable is that it is slow in determining the critical generators. The results section of this dissertation compares the total energy algorithm with the angle, Lagrangian, and Effort. Here we see that the angle algorithm proposed in [19] is more suitable for use in determining the critical generators since it is much faster then the total energy algorithm.

Compared with the Lagrangian we see that it is slower to respond. One of the major differences lies in the fact that the kinetic energy is at a maximum on the largest swing when the potential energy is at its highest absolute value. Since the kinetic energy is squared, it doesn't tell us if the generator is speeding up or slowing down. So looking at the potential energy we see that when it is most negative, it must be at a higher rotor angle, thus accelerating. Thus negating the potential would mean the Lagrangian would be greater at this point then the total energy. At this point the Lagrangian would be at a maximum where as the total energy is not, making the Lagrangian a faster algorithm for detecting the instability. Looking at the case where the fault is near the generator we see that the kinetic energy plays a much more significant role then the potential energy during the fault on case. For faults electrically farther away this is not the case.

CHAPTER 3 LAGRANGIAN AND EFFORT

3.1 INTRODUCTION

The Lagrangian gives us the difference rather then the sum of the energy components. By integrating this difference over time, we find the Action, or Effort. Apart from its use as a clever way to find the Newtonian equations of motion, it has no other physical meaning. Since we integrate it to find the Effort, we can simply think of it as the density or intensity of Effort. The Lagrangian is applied in the same manner as the total energy and as such we treat it as a Lyapunov function.

The Effort on the other hand represents the minimal amount of action that the system takes from one point in time to another. This is difficult to determine since data on whether or not a line was tripped due to a fault may not be available. We first test the system assuming we know these times, and then we implement a new approach by comparing the Lagrangian of the whole system.

3.2 FORMULATION

Looking at the difference between the kinetic energy, and potential energy we form the Lagrangian as shown in 3.1,

$$L_i = KE_i - PE_i \qquad (3.1)$$

Where KE and PE are the kinetic and potential energy of the i^{th} generator computed in real-time as in 2.6. The Effort is then computed by 3.2,

$$E_{effort_i} = \int_{t1}^{t2} L_i dt \qquad (3.2)$$

The integration limits from t1 to t2 represent the time frame in which the Effort of the system is of interest. This time frame is represented as the fault on time for transients dealing with faults.

A new way of determining t1 and t2 is by looking at the system wide Lagrangian, which is simply the sum of the Lagrangians evaluated for each machine. From simulations it is obvious that small changes in load, say +/- 5%, have little effect on the total energy of the system. The effects on the Lagrangian are therefore negligible. A good question to ask is at what point we should declare the system to be in a state of emergency. The short answer to this lies in good engineering judgment at this point rather then mathematical formulation. Further research is needed for theoretical analysis. From simulation on the 39 bus test system, it was found that a value of around 0.2 pu energy indicated severe problems with the system. A justification of using 0.2 pu of energy is shown below where we examine an unstable fault scenario and a stable case where load is changed in the system.

Figure 3- 1: System Lagrangian, Unstable Fault Case

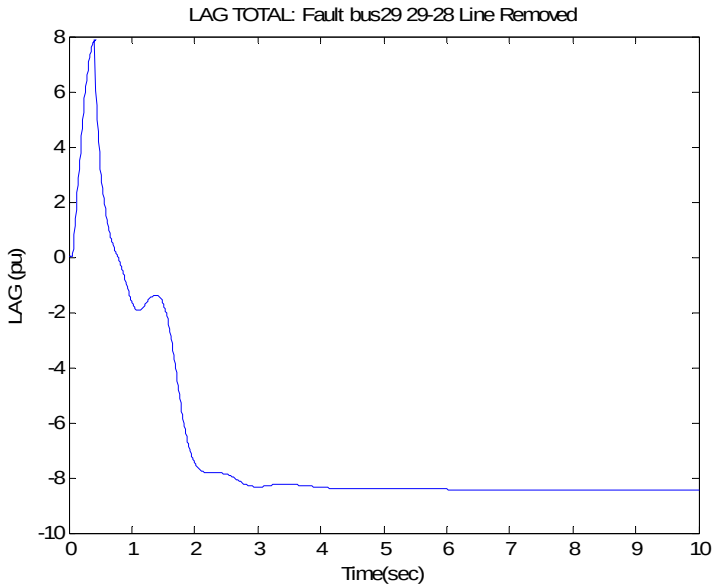

In Figure 3-1 we see that the Lagrangian reaches a maximum of about 8 pu indicating a large disturbance has occurred. For a load change in the system we see in Figure 3-2 that 0.2 pu is a more conservative threshold.

Figure 3- 2: Computation of Lagrange for each generator, no fault simulated

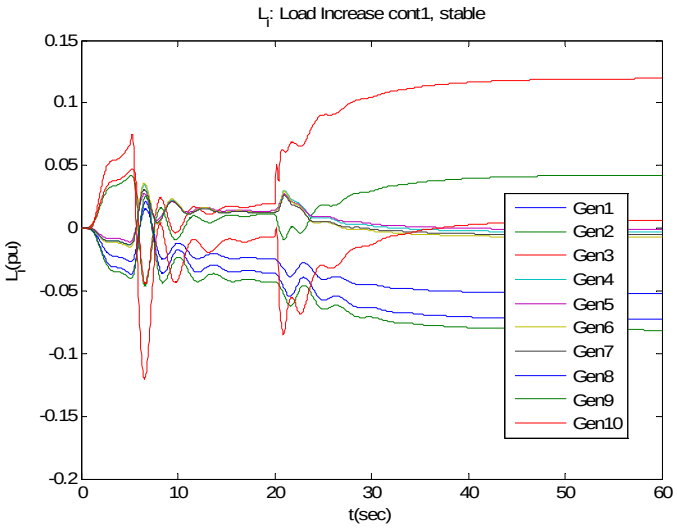

From Figure 3-2, we observe that the Lagrangian for the most effected generator goes to about 0.15. Looking at the sum of L_i over all the individual machines, we see that this sum stays close to zero as shown in Figure 3-3.

Figure 3- 3: Sum of Lagrangians for Cont1, Stable

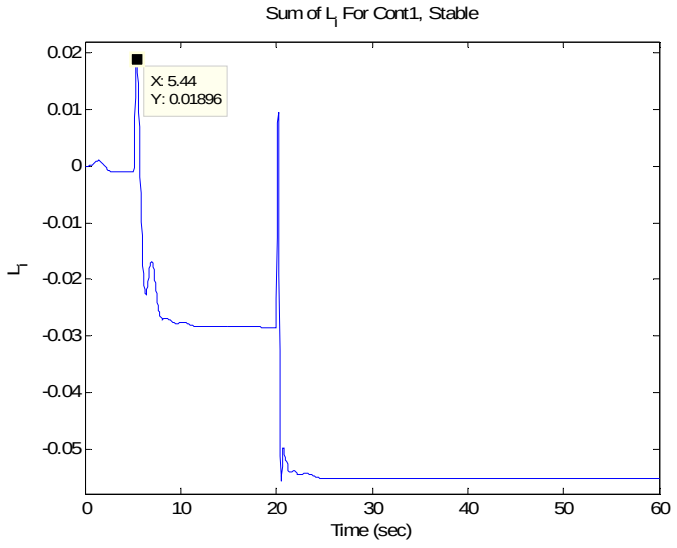

Knowing t1 allows us to define the starting point for the Effort. Let us call this sum TL. Let TL be computed as follows in equation 3.3,

$$TL(t) = \sum_i L_i(t) \qquad (3.3)$$

Equation 3.3 is the same as finding the total energy of a system as described in [7] except we use the Lagrangian.

To determine the ending time t2 we look at the behavior of TL. If TL is decreasing then the phase angle and frequency must be decreasing. At this point, we can conclude that the critical generators are regaining synchronism with the system. If the Effort of the critical machine exceeds the critical amount needed to lose synchronism within the time frame from t1 to t2 then the generator is unstable. If Equation 3.3 begins decreasing before the maximum amount of Effort has been exceeded then we can not say for certain whether the machine will lose synchronism.

3.3 IMPLEMENTATION

To determine the efficiency of the Lagrangian and Effort algorithms we will look at two cases. The first case will include a fault and the other an overloaded system will be simulated with no fault. For the faulted cases the system is stable with regard to +/- 5% load fluctuations. The fault is applied long enough for the system to lose synchronism. The method described above in determining t1 and t2 for use in 3.2 is compared with the method were we assume we know t1 and t2 for a given fault. For simplicity, let us refer to these as method 1 and method 2 respectively. The overloaded system will be analyzed using method 1. A thorough investigation of the Lagrangian and Effort algorithms is left for the results and comparisons section of this dissertation.

For the following fault case, a three phase fault is simulated at bus 4 in the system shown in Figure A-1. Observing the estimated rotor angle, defined on the COI reference frame, in Figure 3-3 below we observe that Generator 3 is the critical generator.

Figure 3- 4: Estimated Rotor Angle from Bus Voltage Angle Measurement

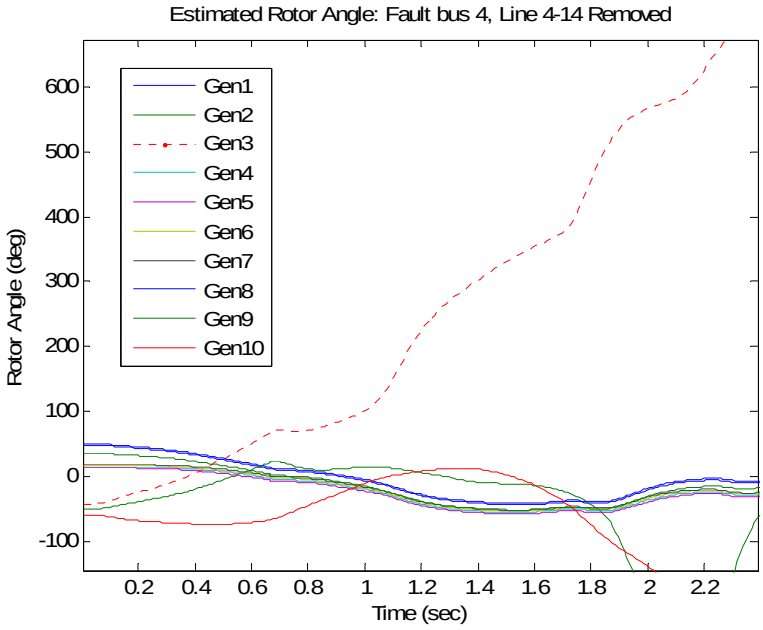

At about 2 seconds, we see that Generators 2 and 10 begin to decelerate from the center of inertia. Area 2, shown in Figure A-1, is clearly losing synchronism with the rest of the system. Computing the load ratio for each area in the system we see that Area 2 has the highest, as shown in Table 3-1 below, thus we shed load at Area 2.

Table 3- 1: Load to Generation Ratio, 39 Bus 3-Area System

Load To Generation Ratio: 39 Bus 3-Area System			
	Area1	Area2	Area3
$Load_i$ (MW)	1647.8	3433	2011.97
Gen_i (MW)	2094.7	2496	2674.3
$Load_i$ / Gen_i	0.787	1.375	0.752
$R_{L/G}$	0.2268	0.4725	0.2769

Determining how much load and generation to trip to make the system stable depends on several factors. Being able to trip generation and load quickly helps in mitigating the angle instability thus the control action time at which each algorithm picks up has a significant effect on how much load should be tripped. For longer control times we need to trip more load and generation to make the system stable. Further research is needed on these important issues. Another factor has to do with the tie-line transfer limits. If, for instance, we decide to trip generation and load at Area 2 but the amount of generation is more then the load then the tie-line connecting Area 2 to the grid becomes more stressed. This problem can be overcome by simply shedding the same amount of load as generation. Using Method 1, the Effort is computed as shown in Figure 3-5.

Figure 3- 5: Effort Computed for method 1

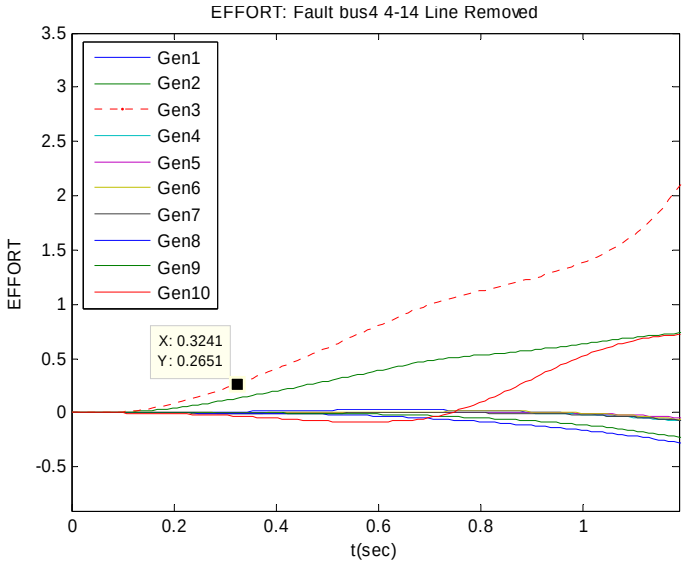

At 0.324 seconds, the Effort of Generator 3 exceeds its critical limit. Generators 2 and 10 begin to pull away from the rest of the system but since Generator 3 was the first to be picked up by the Effort algorithm we shed generation there instead of the other

generators. If we assume we know the fault duration as described in Method 2 we observe a close approximation with the first method. This is shown in Figure 3-6,

Figure 3- 6: Effort Using Method 2

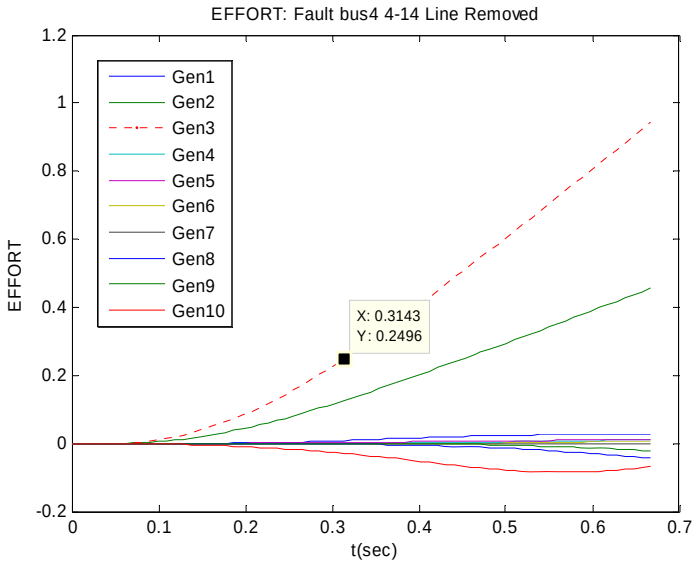

Comparing Figure 3-5 to 3-6 we see that the time difference in picking up Generator 3 is about 0.01 seconds. Figure 3-7 shows the Effort computation for Generator 3 for both methods.

Figure 3- 7: Effort Comparison Between Methods

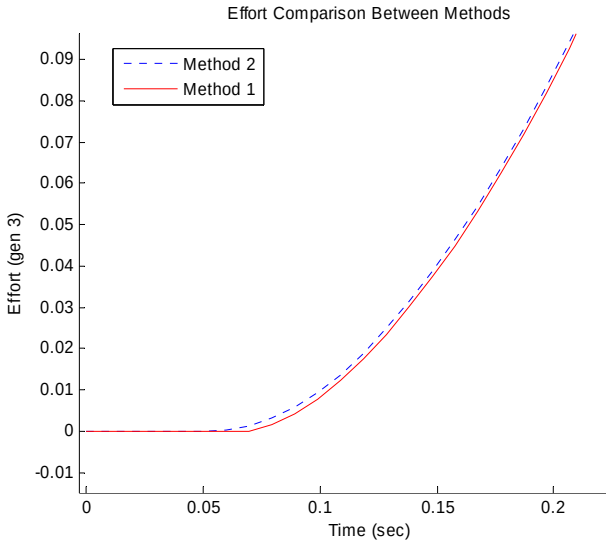

From Figure 3-7 we see graphically that the two methods give almost identical results with little time delay between the two. Comparing the results from the two methods for calculating Effort with those obtained from the other algorithms we see that Effort initiates control action the quickest, as shown in Table 3-2.

Table 3- 2: Control Times Comparisons For Fault At Bus 4

Fault Bus 4, Gen 3 Pickup	
	Control Time(sec)
Method 1	0.324
Method 2	0.314
Lagrange	1.057
TE	1.887
Angle	0.657

3.4 DETERMINING STABILITY LIMITS

For the Lagrangian the limits are determined in exactly the same way as with the total energy. A sustained fault is simulated up until the critical clearing time and we find the maximum value that the machine can withstand. This process is shown in Figure 3-8.

Figure 3- 8: Gen 3 Lagrangian Stability Limit

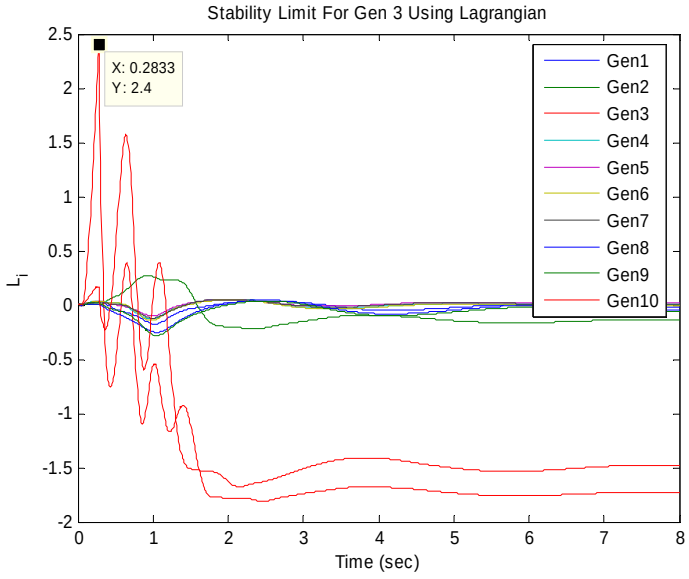

To find the stability limits as given by the Effort, we use the second method. Since we are looking at the simulations to find the limits we can easily determine t1 and t2. For the following simulation shown in Figure 3-9, t1 is 0.05 seconds and t2 is the critical clearing time at 0.283 seconds.

Figure 3- 9: Gen 3 Stability Limit Using Effort

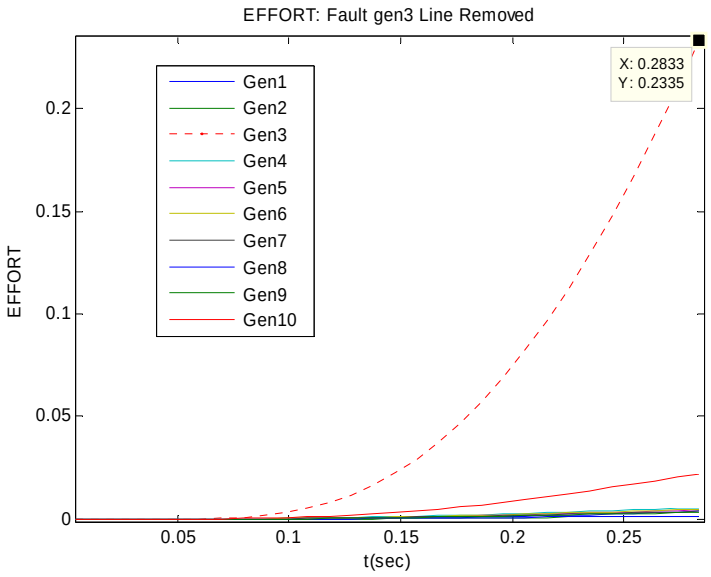

To find the critical Effort for each generator, we look at the Effort computed for the fault on time duration. For Generator 3 we would set this limit to 0.233 as shown in Figure 3-9. This procedure is fairly accurate in determining the limits as long as the loading in the system stays within a reasonable level for which the thresholds were computed on. For changes as much as 20 percent of the total load demand, we need to find a new set of thresholds. In the results section, we look at three load levels, light, medium and heavy and compare the results between each.

3.5 CONCLUSIONS

The Lagrangian appears to be a good measure of stability. Its use in determining instability seems to be comparable to the other algorithms and even indicates instability

faster then the total energy. Since both frequency and estimated rotor angle data is available in real-time from PMU's, it can be quickly computed. For the computation of the energy components, it is necessary that the data be continuous. Any discontinuities can have an impact on the computations resulting in incorrect control actions. Filtering the data using a low pass filter helps in reducing the effects of any discontinuities and has been shown to have only a minor impact on the speed of detecting angle instability.

Although tripping the same amount of generation as load is a good way to insure that the transfer limits are not exceeded, it may not be optimal in terms of lost revenue. After all, tripping less load while shedding more generation would lead to less revenue being lost. A sensible question to ask is how we can lower the amount of load tripped and at the same time maximize the amount of generation tripped in order to keep the system stable. Load shedding schemes developed in [9][10][11][12] along with countless others deal with optimizing load shedding. A lot of these schemes are well suited for special cases but not for large power grids like the eastern interconnection.

Overvoltage is also a key issue in load shedding. In the August 2003 blackout load shedding actually made the situation worse due to the over voltage conditions causing over voltage relays to trip. By tripping less load or by splitting up the amount to trip over a period of time would have alleviated the over voltage conditions. For simplicity, it is assumed that over voltage is not a problem with regards to testing the algorithms. In future research, this issue should be studied in greater detail.

CHAPTER 4 ANGLE MITIGATION ALGORITHM

4.1 INTRODUCTION

The angle algorithm uses a heuristic approach to predicting angle instability based upon observations of the angle trajectories during stable and unstable contingencies. When the rotor angle trajectory exceeds the critical angle θ_c, w.r.t. center of inertia, we then integrate over time the rotor angle. If this integral remains bounded by some predefined quantity then we say that the system is transient stable [19]. Four thresholds, two for the acceleration and deceleration critical angles and two for their time integrals are required for each generation unit. The physical interpretation of the integral is that it represents the generation reserve. Knowing if this reserve is used up during a disturbance is a good indication of the angle stability of the system. Generators with a higher reserve are generally more stable following disturbances [13].

Several advantages from using the angle algorithm include speed of instability detection as well as ease of implementation. Since all trajectories are measured in real-time through PMU's, we can use the algorithm in real-time as well. The estimation of spinning reserve can be updated by noting the change in active power output which can be computed easily from the synchrophasor measurements. For simulations on the New England 39 bus test systems, we use a fixed threshold for the rotor angle θ_c and it's integral denoted as Ω.

Although the angle algorithm is fast, it has shown to be over sensitive as we will see from the simulations. This may be because of the fact that the thresholds need better tuning and because the generation reserves have not been computed accurately enough.

For systems of reasonable size, say 50k buses, we would have to use more sophisticated methods to determine the thresholds.

4.2 FORMULATION

The trigger for initiating the computation of the angle algorithm is given by the maximum deviation from the center of inertia in Equation 2.2. The integral of the rotor angle is denoted by Ω_a and Ω_d for acceleration and deceleration respectively and is computed when the critical angle deviation of Equation 2.2 is exceeded. If θ_i starts decreasing (decelerating) before Ω_a is exceeded then we reset the integral to zero. Conversely if θ_i increases before Ω_d is exceeded then Ω is reset. For the simulations in this dissertation we set Ω_a=2.5 and Ω_d=-2.5.

4.3 IMPLEMENTATION

The implementation on the New England 39 bus system compared with the other algorithms is covered in greater detail in the Results and Comparisons section. Here we will look at the case for a fault at bus 4 with the transmission line connecting bus 4 to bus 14 disconnected to clear the fault. Let us first examine the estimated rotor angles defined on the COI given in Equation 2.2, shown if Figure 4-1 below, simulated on the 3 area New England system shown in Figure A-1. Load shedding is initiated as described in Chapter 3 where Area 2 is given as the best candidate.

Figure 4- 1: Estimated Rotor Angle From Voltage Angle

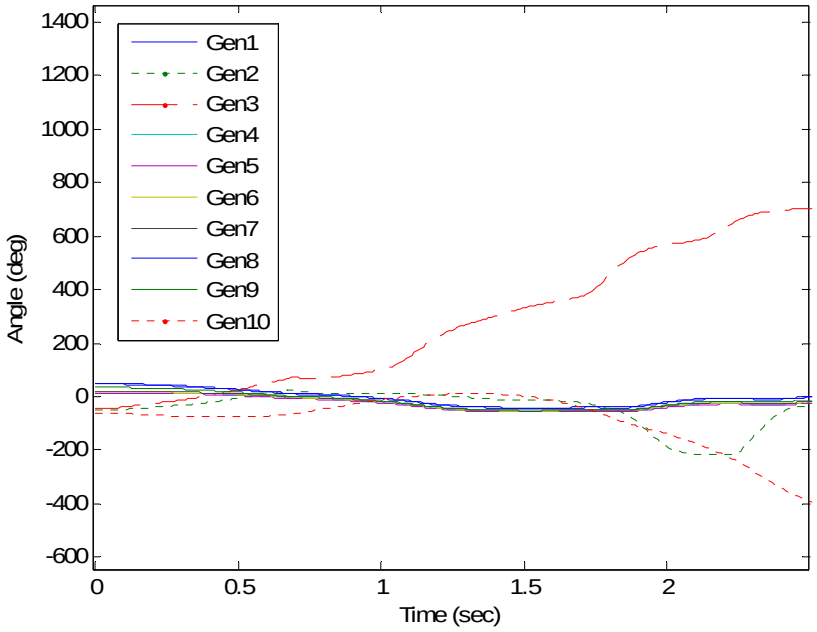

The Generators in Area 2 are at first accelerating from the center of inertia however Generators 2 and 3 stay in synchronism with the system for a longer time. Clearly we need to shed load and generation in Area 2 as Figure 4-1 shows. The area where load shedding should occur is not as obvious until about 1.75 seconds. Looking at the load to generation ratio, given in Table 3-1, at the time of generation shedding gives us a good idea of what area to shed load at will have a highest impact on transient stability.

4.4 CONCLUSIONS

One of the main issues arising from using the angle algorithm is being able to properly determine the spinning reserves, and thus properly setting the maximum integral limit. This can be accomplished using the operating the real power output and estimating the maximum generation output through offline studies.

Determining the critical groups of generators during a disturbance has been shown for the most part to be one of the strong points of using the angle algorithm, as the results in Chapter 5 will show. The tendency of the angle algorithm to over react is another issue that needs to be addressed in future research.

CHAPTER 5 RESULTS AND COMPARISONS

5.1 NEW ENGLAND 39 BUS TEST SYSTEM FAULT CASE

The following tests were done on the original 39 bus system shown in Figure A-2 in the appendix. The thresholds for each algorithm for this case are given in Table 5-1. The maximum limits are given in per unit. In several cases the energy and Lagrange limits are almost identical. For these cases the energy is largely kinetic thus the energy and Lagrangian are almost the same. The spinning reserve integration bounds used in the angle algorithm were set to 2pu.

Table 5- 1: Unmodified 39 Bus System Thresholds

Thresholds For Unmodified 39 Bus System					
	Lagrangian	Effort	Energy	Angle(deg)	Output(MW)
gen1	11.7463	0.407	12.0478	+/-80°	317.82
gen2	2.5737	0.328	2.5935	+/-80°	760.16
gen3	3.4679	0.428	3.147	+/-80°	826.33
gen4	2.9997	0.476	4.2065	+/-80°	803.45
gen5	1.5347	0.303	1.0928	+/-80°	645.81
gen6	2.101	0.45	2.3051	+/-80°	826.33
gen7	2.589	0.592	1.4071	+/-80°	711.92
gen8	2.6268	0.517	1.5786	+/-80°	686.49
gen9	2.8042	0.156	2.1467	+/-80°	1055.17
gen10	15.8196	1.198	20.0394	+/-80°	1271.28

Table 5-2, shown below, compares the algorithms between different fault scenarios. Between the Lagrangian, Effort, and angle algorithm we see a strong correlation between algorithms with regards to correctly indicating the most severe generator. In most cases all four algorithms correctly picked up the candidate generator. We can see from the control times that the Lagrangian and energy algorithms are the slowest while the Effort is comparable with the angle algorithm.

Table 5- 2: Control Times For Unmodified 39 Bus System

39 Bus Original System Fault Cases																	
Unstable Cases								Stable Cases									
Bus 4 4-14								Bus 4 4-14									
Li		Angle Alg		Effort		Energy		Li		Angle Alg		Effort					
2	1.954	2	1.3761	2	1.665	2	2.164	gen2	INF	gen2	INF	2	INF				
3	1.885	3	1.3661	3	1.665	3	2.074	gen3	INF	gen3	INF	3	INF				
Bus 14 4-14								Bus 14 4-14									
Li		Angle Alg		Effort		Energy		Li		Angle Alg		Effort					
8	1.083	1	0.7752	9	0.378	5	1.333	2	INF	1	INF	9	INF				
9	0.825	8	0.4969			6	1.443	3	INF	8	INF						
		9	0.6261			7	1.373	8	0.33	9	INF						
						8	1.333	9	INF								
Bus 5 5-6								Bus 5 5-6									
Li		Angle Alg		Effort		Energy		Li		Angle Alg		Effort					
2	1.421	2	0.7951	2	1.034	2	1.63	2	0.75	2	INF	2	INF				
3	1.65	3	1.5703			3	1.829	3	INF	3	INF						
Bus 25 2-25								Bus 25 2-25									
Li		Angle Alg		Effort		Energy		Li		Angle Alg		Effort					
4	2.333	4	0.339	4	0.568	4	2.773	6	INF	6	INF	6	INF				
5	2.333	5	0.688					7	INF	7	0.88	7	INF				
Bus 2 2-25																	
Li		Angle Alg		Effort		Energy											
6	1.566	6	1.1567	6	1.396	6	1.815										
7	2.014	7	0.8177			7	1.954										
Bus 16 16-21																	
Li		Angle Alg		Effort		Energy											
8	2.473	8	0.2985	8	0.995	5	2.333										
9	0.597	9	0.5473	9	0.328	9	0.796										

With the stable cases we need to make sure that the algorithms do not initiated control actions. The control times are denoted as infinite to indicate that the algorithms correctly classify the system as stable. To be sure that we do not prematurely take control action we compare the Lagrangian, Effort, and angle algorithms to see if all three determine the same generator. Some of the stable cases do pick up stable generators as being unstable but since the other two algorithms did not pick up that generator we do not initiate generation shedding. Let us examine this case. A stable system following a fault at bus 8 with transmission line connecting bus 8 to 9 tripped shows an unstable generator at bus 2. Assuming we know nothing about the stability of the system at that time we

check the output for the other two algorithms and since neither one has confirmed that Generator 2 is unstable we do nothing. Using the control times given in Table 5-2, we see that the critical clearing times improve, shown in Table 5-3.

Table 5- 3: Critical Clearing Time Using Effort Control Times

Fault	Line Removed	CCT (cycles) No Controls	CCT Effort	CCT Angle	CCT Lagrangian	CCT Energy
4	4to14	50	50.8	52.3	51.3	51
14	4to14	32	38.2	38.4	34	34.9
4	4to5	50	50.8	53.1	48	47.6
3	3to4	97	101.12	99	98.2	96.1
4	3to4	50	50.8	52.3	50.6	50.5
5	5to6	41	46.6	45.7	42.7	41.2
6	5to6	37	42.8	43.34	41.1	39.7
2	2to25	51	53.4	54.2	51.9	52
25	2to25	27	39	35	33.2	31
16	16to21	76	76.4	78	76.2	76

The critical clearing time improvement various significantly between different generators as shown in Table 5-3. One reason for this is that the amount of generation shed was set to 50% of the generation active power output which varies by as much as 500 MW as can be seen in Table 5-1. Naturally, the more load and generation removed from the system the less stressed the transmission network becomes. Shedding too much load on the other hand can lead to instability as well so should be avoided.

5.1.1 New England 39 Bus Test System Overloaded Case

Here we examine contingencies involving high loading in the system along with transmission line and generator outages due to over heating. The unstable cases are examined first. The contingencies where arbitrarily chosen to test the algorithms on various operating conditions. Refer to Table A-1 in the appendix for exact contingencies

details. For the first contingency only load increases with line outages are simulated. In these cases, we increase the loading in one area and generation in a different area to simulate an increase in tie-line transfers. Generator 3 is the first to go unstable as can be seen from examining the estimated rotor angles in Figure 5-1 below,

Figure 5- 1: Rotor Angle Estimated From Bus Voltage Angle

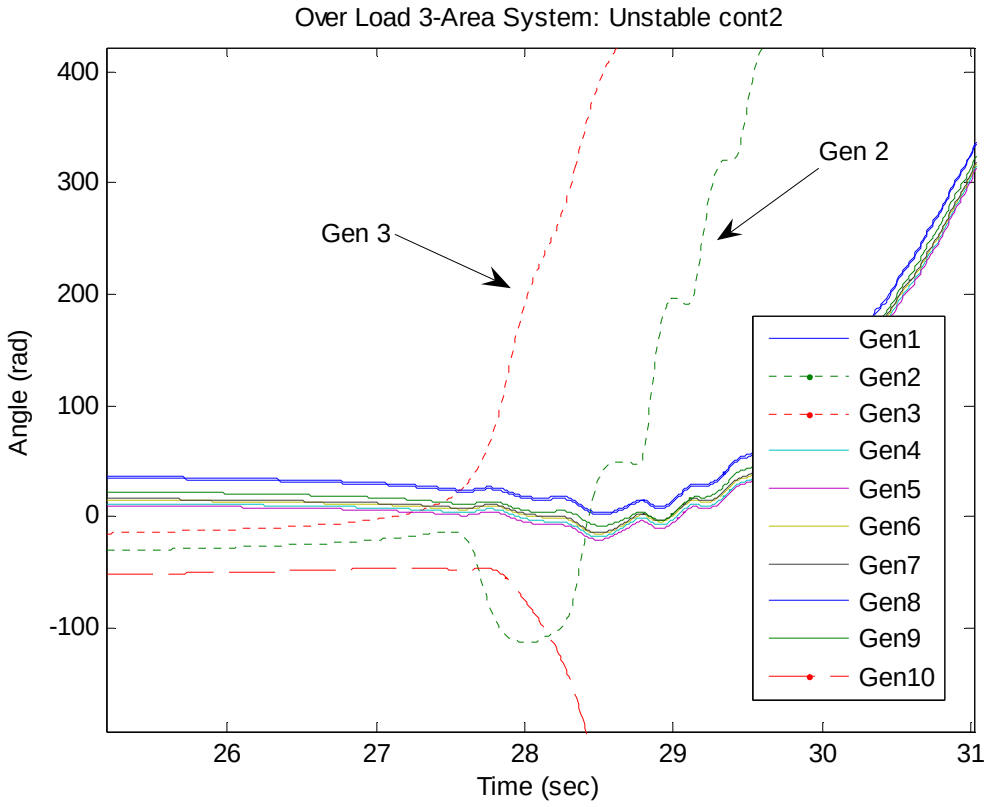

The angle of Generator 3 is the first to increase beyond 90°s and the angle algorithm detects instability at about 28 seconds. Generator 2 stays in synchronism with Generator 10 for about 1 second indicating that the load shedding should occur near Generators 10 and 2. We now look at the other algorithms to determine stability. The Effort isn't computed until the total system energy or Lagrangian exceeds 0.2 pu so to determine stability using Effort we must wait a minimum of 27 sec as shown in Figure 5-2.

Figure 5- 2: Total System Lagrangian for Unstable Cont2

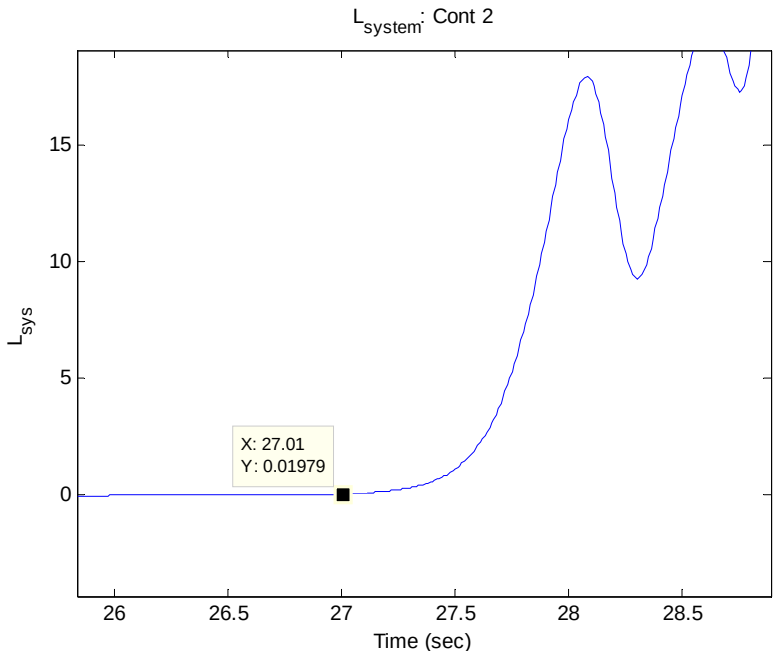

At 27, seconds we begin computing the Effort until the total energy decreases which occurs at 28.25 seconds. The Effort computed within this time period is shown in Figure 5-3.

Figure 5- 3: Effort for Unstable Cont2

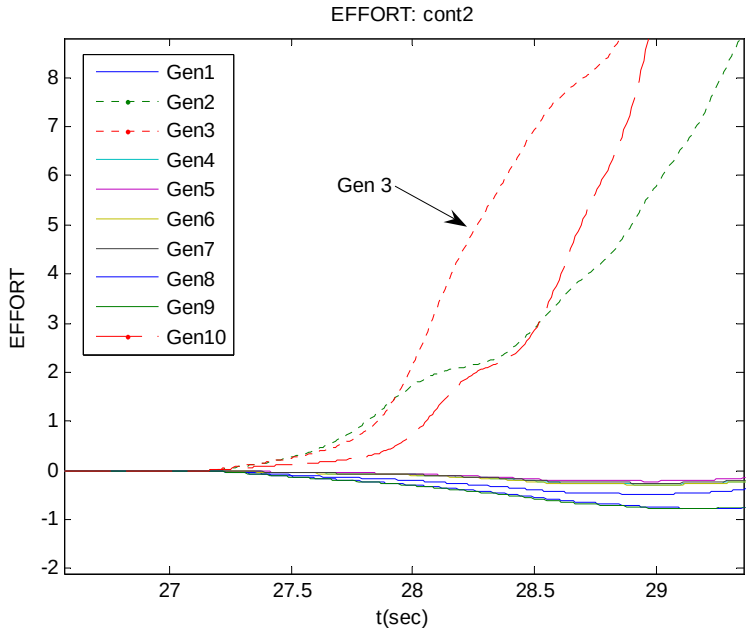

The Effort of the other 9 generators is negligible compared with Generators 2, 3, and 10. Since Generator 3 exceeds its stability threshold first, we shed generation at that unit. The system Lagrangian and total energy are shown in Figure 5-4 and 5-5 respectively.

Figure 5- 4: Lagrange Computation for Unstable Cont1

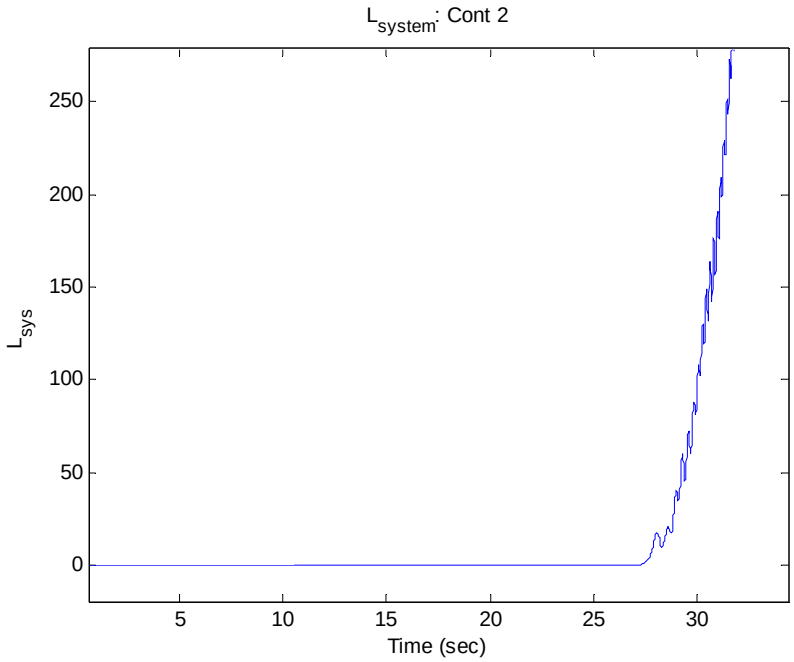

Figure 5- 5 Energy for Unstable Cont1

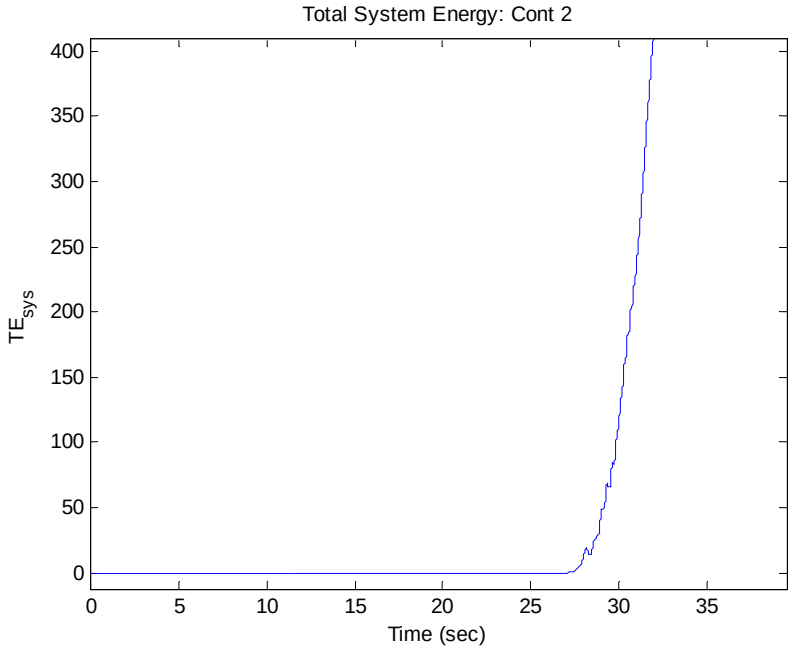

In this case, we see that all four algorithms detected the correct critical set of generators however, since Generators 2 and 3 are electrically close to each other it becomes difficult to tell which one is the most critical.

Table 5- 4: Unstable Cont 1 Algorithm Comparisons

Unstable Cont 1		
	Gen	Time (sec)
Effort	3	27.49
Energy	2	27.73
Lagrange	2	27.65
Angle	2	27.74

Table 5- 5: High Loading Level Comparisons

Unstable Cont 1			Stable Cont 1		
	Gen	Time (sec)		Gen	Time (sec)
Effort	9	7.7	Effort	-	INF
Energy	5	23.02	Energy	-	INF
Lagrange	9	9.27	Lagrange	-	INF
Angle	8	5.69	Angle	-	INF
Unstable Cont 2			Stable Cont 2		
	Gen	Time (sec)		Gen	Time (sec)
Effort	3	27.49	Effort	-	INF
Energy	2	27.73	Energy	-	INF
Lagrange	2	27.65	Lagrange	-	INF
Angle	2	27.74	Angle	-	INF
Unstable Cont 3			Stable Cont 3		
	Gen	Time (sec)		Gen	Time (sec)
Effort	9	20.63	Effort	-	INF
Energy	2	25.36	Energy	-	INF
Lagrange	3	25.52	Lagrange	-	INF
Angle	8	6.04	Angle	-	INF
Unstable Cont 4			Stable Cont 4		
	Gen	Time (sec)		Gen	Time (sec)
Effort	9	24.870001	Effort	-	INF
Energy	5	50.23	Energy	-	INF
Lagrange	9	30.93	Lagrange	-	INF
Angle	8	21.11	Angle	-	INF

In the previous case, we see that the Effort, energy, and Lagrangian indicated instability quickly and at almost the same time. The Lagrangian is actually the quickest to indicate the critical generator where as in the fault case we saw that Effort and the

angle algorithm were the quickest. One important aspect of using energy is that both angle and frequency is used making it more flexible in determining stability among many different scenarios. Table 5-5 shows the comparisons of 4 stable and unstable Contingencies.

The stable cases show that none of the algorithms initiated a false trip. Since neither the total energy of the system or total Lagrangian of the system exceeded 0.2 pu an event was not detected thus Effort was not computed for any of the four stable contingencies. Other algorithms are used in power systems to detect when an event is occurring, such as frequency decline, however since we are calculating energy it is easy to check and see if it is changing significantly which would indicate an event. The Lagrangian shown in Figure 5-6 clearly shows that each generator settles down to its stable equilibrium.

Figure 5- 6: Lagrangian for Stable Cont 4

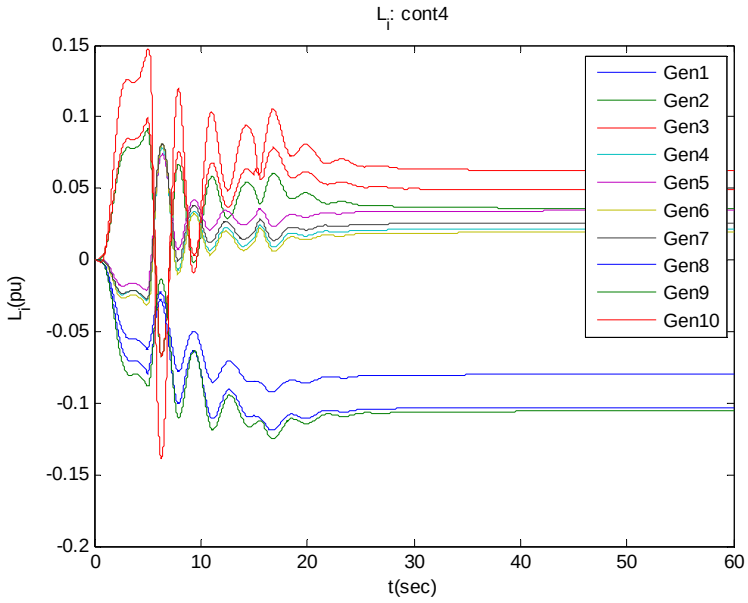

5.2 39 BUS 3 AREA SYSTEM FAULT CASE

The simulations for the 39 bus test system separated into 3 areas connected through long transmission tie-lines as shown in Figure A-1 in the appendix. As with the previous test system, we look at cases where faults cause instability and also for heavy loading scenarios. Tables 5-6, 5-7, and 5-8 show the thresholds for various loading levels of the system. These correspond with maximum loading with decrements of 20% of the maximum.

Table 5- 6: Max Loading Thresholds

	Thresholds, Max Loading				
	Effort	Lagrange	Energy	Angle(deg)	Output(MW)
gen1	0.15	1.5971	1.6644	+/-90°	496.19
gen2	0.5	2.1816	2.8869	+/-90°	608.92
gen3	0.23	2.4005	2.6179	+/-90°	698.81
gen4	0.37	2.1046	2.4125	+/-90°	666.65
gen5	0.35	1.125	1.1854	+/-90°	535.85
gen6	0.34	2.1156	2.4022	+/-90°	685.69
gen7	0.46	1.7097	1.9052	+/-90°	590.70
gen8	0.15	2.0554	2.1241	+/-90°	674.58
gen9	0.07	1.4012	1.5821	+/-90°	770.45
gen10	1.02	9.3675	11.4086	+/-90°	1054.41

Table 5- 7: Thesholds For 20% Less Load

	Thresholds, Minus 20% Load/Generation				
	Effort	Lagrange	Energy	Angle(deg)	Output(MW)
gen1	0.28	1.0468	1.045	+/-90°	396.93
gen2	0.48	1.9945	2.4465	+/-90°	440.91
gen3	0.29	2.0464	2.237	+/-90°	559.06
gen4	0.41	1.3643	2.2027	+/-90°	533.26
gen5	0.34	0.7266	0.7782	+/-90°	428.65
gen6	0.44	1.3996	1.6653	+/-90°	548.49
gen7	0.47	1.0812	1.3529	+/-90°	472.51
gen8	0.4	1.9316	1.9916	+/-90°	539.65
gen9	0.28	2.5159	2.745	+/-90°	616.33
gen10	1.56	10.9976	14.1353	+/-90°	843.57

Table 5- 8: Thresholds For 40% Less Load

	Thresholds, Minus 40% Load/Generation				
	Effort	Lagrange	Energy	Angle(deg)	Output(MW)
gen1	0.27	0.5547	0.9211	+/-90°	297.65
gen2	0.35	1.9453	2.386	+/-90°	309.75
gen3	0.35	1.6131	2.3881	+/-90°	419.22
gen4	0.47	1.214	2.3556	+/-90°	399.88
gen5	0.25	0.4158	0.4527	+/-90°	321.43
gen6	0.52	1.3773	2.201	+/-90°	411.27
gen7	0.34	1.5521	2.1847	+/-90°	354.33
gen8	0.42	1.0989	1.621	+/-90°	404.68
gen9	0.53	2.2245	2.4637	+/-90°	462.17
gen10	1.34	8.3141	13.9735	+/-90°	632.61

Generation has been scaled by the same amount as the load. It should be noted that the angle algorithm thresholds were increased to 90° for simulations on the 3 area 39 bus system to reduce its sensitivity to false instability indication.

The tests on the 39 bus 3-area power system include testing three different thresholds, calculated at the 3 loading levels, to determine the algorithms effectiveness in correctly indicating instability with regards to moderate and large load changes. The thresholds used are indicated in the first column of Tables 5-9, 5-10, and 5-11. The actual loading level is indicated in the header of each table. The angle algorithm thresholds are held at 90° for all loading cases.

Table 5- 9: Unstable Cases Using Maximum Loading

Unstable Cases: Max Loading								
	Bus 4 4-14							
Threshold	Energy Function		Angle Alg		Lagrange		Effort	
Max	2	1.887	3	0.657	2	2.047	3	0.34
	3	1.267	10	0.119	3	1.057		
-20%	2	1.887			2	2.037	3	0.37
	3	1.257			3	0.637		
-40%	3	1.267			2	2.037	2	0.6
	5	1.087			3	0.304	3	0.4
	Bus 5 5-6							
Threshold	Energy Function		Angle Alg		Lagrange		Effort	
Max	2	0.897	3	0.579	2	0.393	2	0.44
	3	0.867	10	0.109	3	0.314	3	0.29

-20%	2	0.877			2	0.314	2	0.43
	3	0.837			3	0.265	3	0.32
-40%	2	0.877			2	0.304	2	0.36
	3	0.847			3	0.216	3	0.34
	5	0.747						
	Bus 12 12-11							
Threshold	Energy Function		Angle Alg		Lagrange		Effort	
Max	2	2.197	3	0.969	2	2.307	3	0.43
	3	2.187	10	0.129	3	1.977		
-20%	2	2.187			2	2.307	3	0.48
	3	2.177			3	1.957		
-40%	3	2.177			2	2.307	2	1.13
	5	1.107			3	1.917	3	0.54
	Bus 21 21-22							
Threshold	Energy Function		Angle Alg		Lagrange		Effort	
Max	2	1.737	2	0.195	6	0.388	6	0.37
	3	1.577	10	0.108	7	3.448		
-20%	2	1.727			6	0.224	6	0.42
	3	1.547			7	0.233		
-40%	2	1.717			5	0.388	7	0.44
	3	1.557			6	0.224		
	Bus 23 23-24							
Threshold	Energy Function		Angle Alg		Lagrange		Effort	
Max	2	1.747	2	0.195	6	3.518	6	0.4
	3	1.587	10	0.108	7	0.195	7	0.37
-20%	2	1.737			6	0.253	6	0.45
	3	1.557			7	0.127	7	0.38
-40%	2	1.737			6	0.253	7	0.32
	3	1.567			7	0.175		
	Bus 24 24-16							
Threshold	Energy Function		Angle Alg		Lagrange		Effort	
Max	2	1.62	2	0.21	2	1.53	6	0.41
	3	1.48	10	0.11	3	1.44	7	0.5
-20%	2	1.61			6	0.29	6	0.47
	3	1.45			7	0.22	7	0.51
-40%	2	1.61			5	0.45	6	0.51
	3	1.46			6	0.29	7	0.42
	Bus 26 26-28							
Threshold	Energy Function		Angle Alg		Lagrange		Effort	
Max	3	1.547	1	0.166	1	0.233	8	0.28
	9	0.262	8	0.146	9	0.195	9	0.2
-20%	3	1.427			1	0.166	1	0.34
	9	0.339			9	0.262	9	0.31
-40%	1	0.233			1	0.118	1	0.33
	9	0.32			8	0.195	9	0.39
	Bus 26 26-29							
Threshold	Energy Function		Angle Alg		Lagrange		Effort	

Max	9	0.262	8	0.146	1	0.233	1	0.26
			10	0.118	9	0.195	9	0.2
-20%	9	0.339			1	0.166	1	0.34
					9	0.262	9	0.31
-40%	1	0.233			1	0.118	1	0.33
	9	0.32			8	0.195	9	0.39
	Bus 29 29-28							
Threshold	Energy Function		Angle Alg		Lagrange		Effort	
Max	9	0.243	8	0.166	9	0.156	1	0.33
			10	0.127			9	0.18
-20%	9	0.301			1	0.497	9	0.27
					9	0.224		
-40%	9	0.282			1	0.156	1	0.45
					9	0.204	9	0.34

Table 5- 10: Unstable Cases Using 20% Less Load Of Maximum

Unstable Cases: -20% Load/Generation								
	Bus 4 4-14							
Threshold	Energy Function		Angle Alg		Lagrange		Effort	
Max	2	2.25	2	2.18	3	1.53	3	0.42
	3	1.43	3	0.75				
-20%	2	2.23			3	1.52	3	0.47
	3	1.42						
-40%	2	2.23			3	1.51	3	0.52
	3	1.43						
	Bus 5 5-6							
Threshold	Energy Function		Angle Alg		Lagrange		Effort	
Max	2	1.25	3	0.63	2	1.07	2	0.67
	3	1.19	10	0.39	3	1.02	3	0.35
-20%	2	1.24			2	1.06	2	0.64
	3	1.17			3	1	3	0.39
-40%	2	1.24			2	1.06	2	0.52
	3	1.18			3	0.39	3	0.42
	Bus 12 12-11							
Threshold	Energy Function		Angle Alg		Lagrange		Effort	
Max	2	3.317	2	2.127	2	3.517	2	2.03
	3	2.567	3	1.411	3	2.307	3	0.61
-20%	2	3.297			2	3.507	2	1.97
	3	2.547			3	2.267	3	0.75
-40%	2	3.297			2	3.507	2	1.68
	3	2.557			3	2.107	3	0.89
	Bus 21 21-22							
Threshold	Energy Function		Angle Alg		Lagrange		Effort	
Max	3	1.537	2	0.373	-	-	6	0.46
			6	0.422	-	-	7	0.69
			10	0.304				

-20%	3	1.467			-	-	6	0.53
					-	-	7	0.7
-40%	3	1.497			1	1.237	6	0.59
					5	1.367	7	0.56
	Bus 23 23-24							
Threshold	Energy Function		Angle Alg		Lagrange		Effort	
Max	3	1.577	7	0.314	-	-	6	0.5
			10	0.314	-	-	7	0.46
-20%	3	1.507			7	0.167	6	0.58
							7	0.46
-40%	3	1.537			5	1.437	6	0.65
					7	0.295	7	0.38
	Bus 24 24-16							
Threshold	Energy Function		Angle Alg		Lagrange		Effort	
Max	3	1.757	2	0.393	-	-	6	0.55
			7	0.432	-	-	7	0.7
			10	0.324				
-20%	3	1.677			-	-	6	0.65
					-	-		
-40%	3	1.707			1	1.627	7	0.56
					5	1.497		
	Bus 26 26-28							
Threshold	Energy Function		Angle Alg		Lagrange		Effort	
Max	1	0.827	1	0.285	1	0.737	1	0.3
	9	0.324	8	0.246	9	0.246	9	0.23
			9	0.353				
-20%	1	0.777			1	0.226	1	0.42
	9	0.539			9	0.363	9	0.36
-40%	1	0.767			1	0.138	1	0.41
	9	0.451			9	0.334	9	0.46
	Bus 26 26-29							
Threshold	Energy Function		Angle Alg		Lagrange		Effort	
Max	1	0.847	1	0.285	1	0.747	1	0.3
	9	0.324	8	0.246	9	0.246	9	0.23
			9	0.353				
-20%	1	0.787			1	0.226	1	0.42
	9	0.539			9	0.363	9	0.36
-40%	1	0.767			1	0.138	1	0.41
	9	0.451			9	0.334	9	0.46
	Bus 29 29-28							
Threshold	Energy Function		Angle Alg		Lagrange		Effort	
Max	1	0.887	1	0.383	1	0.807	1	0.46
	9	0.285	8	0.334	9	0.207	9	0.2
			9	0.314				
-20%	1	0.837			1	0.727	9	0.32
	9	0.402			9	0.295		
-40%	1	0.827			1	0.667	1	0.69
	9	0.373			9	0.275	9	0.4

Table 5- 11: Unstable Cases With 40% Less Load From Maximum

Unstable Cases: -40% Load/Generation								
	Bus 4 4-14							
Threshold	Energy Function		Angle Alg		Lagrange		Effort	
Max	-	-	2	1.637	-	-	2	1.74
	-	-	3	1.178	-	-	3	0.55
-20%	-	-			-	-	2	1.7
	-	-			-	-	3	0.65
-40%	1	2.854			3	3.513	2	1.45
	5	2.126					3	0.78
	Bus 5 5-6							
Threshold	Energy Function		Angle Alg		Lagrange		Effort	
Max	2	1.407	3	0.781	2	1.257	2	0.85
	3	1.387	10	0.169	3	1.257	3	0.4
-20%	2	1.397			2	1.247	2	0.81
	3	1.377			3	1.237	3	0.46
-40%	2	1.387			2	1.227	2	0.63
	3	1.357			3	1.177	3	0.51
	Bus 12 12-11							
Threshold	Energy Function		Angle Alg		Lagrange		Effort	
Max	3	5.16	3	3.44	2	5.34	3	0.94
			10	5.6	3	4.96	10	2.22
-20%	3	5.15			2	5.32	2	2.21
					3	4.9	3	1.13
-40%	3	5.14			2	5.28	2	1.74
					3	4.67	3	1.3
	Bus 21 21-22							
Threshold	Energy Function		Angle Alg		Lagrange		Effort	
Max	9	1.37	2	0.36	9	1.34	6	0.6
	1	1.45	10	0.22			7	0.92
			6	0.48				
-20%	1	1.28			1	1.31	6	0.72
	3	1.45					7	0.93
-40%	1	1.2			5	1.04	6	0.82
	2	1.48			1	1.19	7	0.75
	Bus 23 23-24							
Threshold	Energy Function		Angle Alg		Lagrange		Effort	
Max	1	1.63	2	0.4	-	-	6	0.71
	3	1.67	7	0.34	-	-	7	0.57
			10	0.24				
-20%	1	1.45			1	1.49	6	0.85
	3	1.61			7	0.28	7	0.58
-40%	1	1.36			4	1.16	6	0.96
	3	1.57			5	1.11	7	0.46
	Bus 24 24-16							

Threshold	Energy Function		Angle Alg		Lagrange		Effort	
Max	3	1.69	2	0.42	-	-	6	0.83
			7	0.51	-	-	7	0.98
			10	0.28				
-20%	1	1.62			-	-	6	0.99
	3	1.64			-	-	7	0.99
-40%	1	1.43			1	1.35	7	0.79
	3	1.59			5	1.54		
	Bus 26 26-28							
Threshold	Energy Function		Angle Alg		Lagrange		Effort	
Max	1	1.07	8	0.19	1	1.03	1	0.36
	9	0.55	9	0.33	9	0.36	9	0.27
-20%	1	1.06			1	1.02	1	0.56
	8	1.24			8	1.09	9	0.43
-40%	1	1.05			1	0.17	1	0.53
	5	0.66			9	0.44	9	0.56
	9	1.49						
	Bus 26 26-29							
Threshold	Energy Function		Angle Alg		Lagrange		Effort	
Max	1	1.07	8	0.19	1	1.03	1	0.36
	9	0.55	9	0.33	9	0.36	9	0.27
-20%	1	1.06			1	1.02	1	0.56
	8	1.25			8	1.1	9	0.43
-40%	1	1.05			1	0.17	1	0.53
	5	0.66			9	0.44	9	0.56
	8	1.2						
	Bus 29 29-28							
Threshold	Energy Function		Angle Alg		Lagrange		Effort	
Max	1	1.81	8	0.27	1	1.75	1	0.45
	9	1.52	9	0.28	9	0.13	9	0.14
-20%	1	1.8			1	1.06	1	0.74
	9	1.55			9	0.3	9	0.26
-40%	1	1.79			1	0.25	1	0.7
	9	1.53			9	0.2	9	0.36

The following tables show some interesting correlations between thresholds and loading levels. For the maximum loading case shown in Table 5-9 the thresholds computed on each of the load levels produced similar results. However, using thresholds computed at a lower loading level on a system with increased load causes the algorithms to be less sensitive. Conversely, if we use thresholds computed on a system that has a greater loading amount then what is actually being used in the system then the algorithm

generally tends to be more sensitive in detecting instability. For load fluctuations that are small, say +/-5% of total load demand, we wouldn't need to update the thresholds. Load fluctuations in excess of +/-20% would mean that a new set of thresholds would need to be used in order to correctly identify critical generators. This should be a concern only in systems operating near maximum loading since faults are usually cleared in much less time than the c.c.t. for lightly loaded systems.

We now compare the improvements in c.c.t. shown in Tables 5-12, 5-13, and 5-14.

Table 5- 12: CCT at Max Loading Using Different Threshold Sets

Simulations At Max Loading					
Simulations Using Thresholds From Max Loading					
Contingency	CCT	Energy	Angle	Lagrange	Effort
bus 4 4-14	33.29	33.43	33.72	33.44	34.6
bus 5 5-6	23.91	24.61	24.9	25.19	25.19
bus12 12-11	63.05	63.06	87.93	63.06	66.82
bus26 26-29	9.80	18.98	16.38	20.14	20.14
bus29 29-28	9.95	19.56	15.34	20.28	20.14
bus26 26-28	10.82	19.13	16.96	20.28	20.28
bus21 21-22	17.80	18.11	30.68	19.7	20
bus23 23-24	17.80	18.26	29.96	21	20
bus24 24-16	22.17	22.59	34.15	22.59	26
Simulations Using Thresholds From -20% Loading					
Contingency	CCT	Energy	Angle	Lagrange	Effort
bus 4 4-14	33.29	33.81	33.72	33.5	33.94
bus 5 5-6	23.91	24.24	24.9	24	24.89
bus12 12-11	63.05	63.1	87.93	64.22	65.94
bus26 26-29	9.80	17.8	16.38	19.54	19.86
bus29 29-28	9.95	18.9	15.34	19.81	19.37
bus26 26-28	10.82	18.5	16.96	19.81	19.34
bus21 21-22	17.80	17.2	30.68	19.2	18.11
bus23 23-24	17.80	18.03	29.96	20.34	19.93
bus24 24-16	22.17	22.25	34.15	21.27	25.52
Simulations Using Thresholds From -40% Loading					
Contingency	CCT	Energy	Angle	Lagrange	Effort
bus 4 4-14	33.29	33.06	33.72	34.95	34.01
bus 5 5-6	23.91	24.14	24.9	24.39	25.24
bus12 12-11	63.05	64.2	87.93	66.9	66.87
bus26 26-29	9.80	17.2	16.38	18.31	19.73
bus29 29-28	9.95	16.76	15.34	18.02	19.24

bus26 26-28	10.82	18.53	16.96	17.36	18.96
bus21 21-22	17.80	18.9	30.68	17.22	17.94
bus23 23-24	17.80	18.47	29.96	18.92	19.17
bus24 24-16	22.17	23.66	34.15	23	24.78

Table 5- 13: CCT at -20% Loading Using Different Threshold Sets

Simulations At -20% Loading					
Simulations Using Thresholds From Max Loading					
Contingency	CCT	Energy	Angle	Lagrange	Effort
bus 4 4-14	51.94	52	52.08	52.11	53.11
bus 5 5-6	34.54	35.94	34.04	34.53	34.97
bus12 12-11	104.67	104.11	104.7	104.45	106.1
bus26 26-29	17.95	23.23	21.87	18.11	23.54
bus29 29-28	18.24	23.19	24.04	22.74	23.74
bus26 26-28	18.67	23.99	24.47	24	25.62
bus21 21-22	24.94	25.14	28.38	-	28.67
bus23 23-24	25.52	25.34	33	-	32.11
bus24 24-16	29.59	30.27	32.86	-	32.64
Simulations Using Thresholds From -20% Loading					
Contingency	CCT	Energy	Angle	Lagrange	Effort
bus 4 4-14	51.94	51.93	52.08	51.93	52.65
bus 5 5-6	34.54	34.59	34.04	34.59	34.88
bus12 12-11	104.67	104.54	104.7	104.54	104.98
bus26 26-29	17.95	24.47	21.87	18.11	23.17
bus29 29-28	18.24	22.74	24.04	22.74	22.74
bus26 26-28	18.67	24.62	24.47	19.27	24.62
bus21 21-22	24.94	24.76	28.38	-	28.09
bus23 23-24	25.52	25.48	33	32.28	29.82
bus24 24-16	29.59	29.53	32.86	-	31.56
Simulations Using Thresholds From -40% Loading					
Contingency	CCT	Energy	Angle	Lagrange	Effort
bus 4 4-14	51.94	51.5	52.08	51.89	52.45
bus 5 5-6	34.54	35.13	34.04	34.25	34.29
bus12 12-11	104.67	104.3	104.7	104.61	104.72
bus26 26-29	17.95	23.92	21.87	18.96	23.33
bus29 29-28	18.24	22.47	24.04	21.49	23.12
bus26 26-28	18.67	24.31	24.47	19.31	24.51
bus21 21-22	24.94	25.1	28.38	26.1	28.23
bus23 23-24	25.52	25.82	33	32.06	32.43
bus24 24-16	29.59	30.75	32.86	31.68	31.97

Table 5- 14: CCT at -40% Loading Using Different Threshold Sets

Simulations At -40% Loading					
Simulations Using Thresholds From Max Loading					
Contingency	CCT	Energy	Angle	Lagrange	Effort
bus 4 4-14	167.80	-	132.88	-	135
bus 5 5-6	49.30	51.05	52.56	50.03	5.22
bus12 12-11	264.90	217.99	218.9	217.69	221.03
bus26 26-29	24.40	30.62	34.8	33.41	32.77
bus29 29-28	26.40	34.19	33.5	35.22	35.82
bus26 26-28	25.00	33.89	35.1	31.76	34.27
bus21 21-22	35.69	49.43	49.5	48.36	49.07
bus23 23-24	39.96	51.97	53.44	-	55.82
bus24 24-16	44.05	58.2	58.97	-	59.34
Simulations Using Thresholds From -20% Loading					
Contingency	CCT	Energy	Angle	Lagrange	Effort
bus 4 4-14	167.80	132.59	132.88	133.01	133.21
bus 5 5-6	49.30	52.36	52.56	50.87	52.67
bus12 12-11	264.90	218.76	218.9	218.32	218.5
bus26 26-29	24.40	30.94	34.8	33.09	32.23
bus29 29-28	26.40	32.37	33.57	35.97	36.9
bus26 26-28	25.00	33.32	35.15	34.11	34.1
bus21 21-22	35.69	46.9	49.5	46.38	49.16
bus23 23-24	39.96	53.54	53.44	52.74	55.89
bus24 24-16	44.05	54.73	58.97	57.35	57.51
Simulations Using Thresholds From -40% Loading					
Contingency	CCT	Energy	Angle	Lagrange	Effort
bus 4 4-14	167.80	132.9	132.88	132.88	134
bus 5 5-6	49.30	51.98	52.56	51.98	52.3
bus12 12-11	264.90	218.9	218.9	218.88	218.9
bus26 26-29	24.40	31.7	34.8	32.77	32.77
bus29 29-28	26.40	32.63	33.5	35.68	36
bus26 26-28	25.00	32.48	35.1	33.35	33.36
bus21 21-22	35.69	48.49	49.5	48.64	49.36
bus23 23-24	39.96	52.41	53.44	52.7	55.47
bus24 24-16	44.05	58.09	58.97	58.1	58.82

In the each of the previous tables the loading in the system is held constant while the threshold sets are varied. The results indicate that each algorithm performs differently between areas as the loading changes. This could be from the stress on the system at high loading being reduced as the loading is reduced. As an example let us examine Table 5-12. The last three cases with faults in Area 1 show that the angle

algorithm has the greatest improvement in critical clearing time, where as in Area 3, the Effort shows a greater improvement over the angle algorithm. The effects load changes have on the thresholds are not clearly understood and further research is needed.

5.2.1 39 BUS 3 AREA SYSTEM HEAVY LOADING CASE

For the heavy loading cases simulated on the 39 bus 3 area system we look at the maximum loaded system as the base load demand. Four stable and unstable cases are shown in Table 5-15. The thresholds computed using offline transient simulations are given in Table 5-6, using the heaviest loading scenario.

Table 5- 15: Excessive Loading, 3-Area System

Unstable Cont 1			Stable Cont 1		
	Gen	Time (sec)		Gen	Time (sec)
Effort	3	29.28	Effort	NAN	INF
Energy	3	29.56	Energy	NAN	INF
Lagrange	3	29.28	Lagrange	NAN	INF
Angle	3	29.68	Angle	NAN	INF
Unstable Cont 2			Stable Cont 2		
	Gen	Time (sec)		Gen	Time (sec)
Effort	3	26.52	Effort	NAN	INF
Energy	3	26.84	Energy	NAN	INF
Lagrange	3	26.6	Lagrange	NAN	INF
Angle	3	26.88	Angle	NAN	INF
Unstable Cont 3			Stable Cont 3		
	Gen	Time (sec)		Gen	Time (sec)
Effort	3	41	Effort	NAN	INF
Energy	3	41.36	Energy	NAN	INF
Lagrange	3	41	Lagrange	NAN	INF
Angle	3	41.36	Angle	NAN	INF
Unstable Cont 4			Stable Cont 4		
	Gen	Time (sec)		Gen	Time (sec)
Effort	3	10.56	Effort	NAN	INF
Energy	3	10.8	Energy	NAN	INF
Lagrange	3	10.52	Lagrange	NAN	INF
Angle	3	10.92	Angle	NAN	INF

The stable cases all indicate that the system remains stable as predicted from all four algorithms. Looking at the unstable cases we see that the four algorithms detect the

critical generators with control times almost identical to each other. It also appears that in the three area system the angle algorithm detects instability better. This could be due to the fact that with higher loading the system in the 3 area case the system is beyond marginally unstable where as in the unmodified system the loading leads to marginal instability with only one generator losing synchronism. The excessive loaded cases do cause the system to break apart as seen from the rotor angle measurements shown in Figure 5-7 below,

Figure 5- 7: Rotor Angle For 3-Area Over Load Case

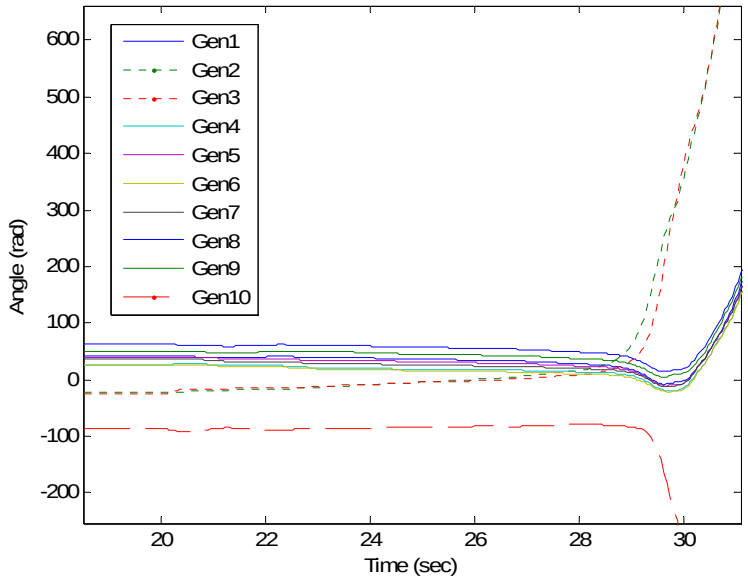

In fact, we see that area 2 loses synchronism from the rest of the system with Generators 2 and 3 accelerating and Generator 10 decelerating. Examining the Lagrangian and Effort we see that both Generator 2 and 3 would be candidates for tripping since they remain in synchronism with each other. The Lagrangian, Energy, and Effort are shown in Figures 5-8, 5-9, and 5-10 respectively.

Figure 5- 8: Lagrangian Computation for Unstable Cont4

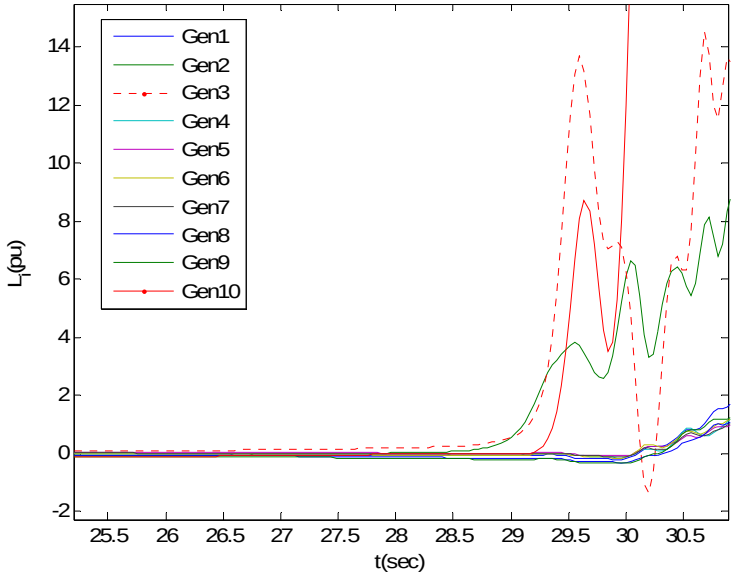

For the Lagrangian, we see little difference between Generator 2 and 3 between 28 and 29.25 seconds. Generator 3 losses synchronism the fastest as you can see from the dotted line in Figure 5-8.

Figure 5- 9: Energy Computation for Unstable Cont4

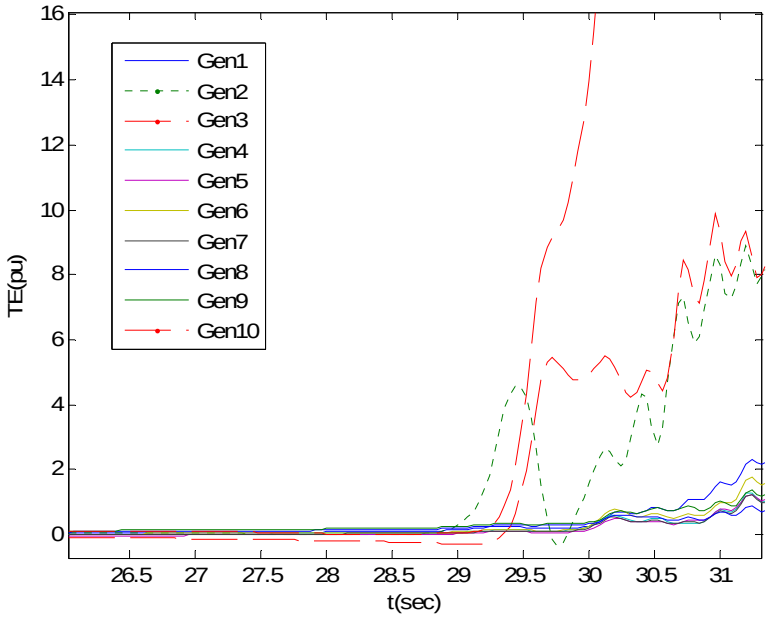

The total energy in Figure 5-9 shows that Generator 2 is the critical generator, rather then Generator 3. This error is due to the kinetic energy not being corrected as explained in [5], were the energy not contributing to the instability should be subtracted out. Without correcting the kinetic energy, we end up with a phase shifted signal as can be observed in Figure 5-9. Correcting for the non contributing kinetic energy is not easily accomplished in real-time since it requires the trajectories to be computed.

Figure 5- 10: Effort Computation Unstable Cont4

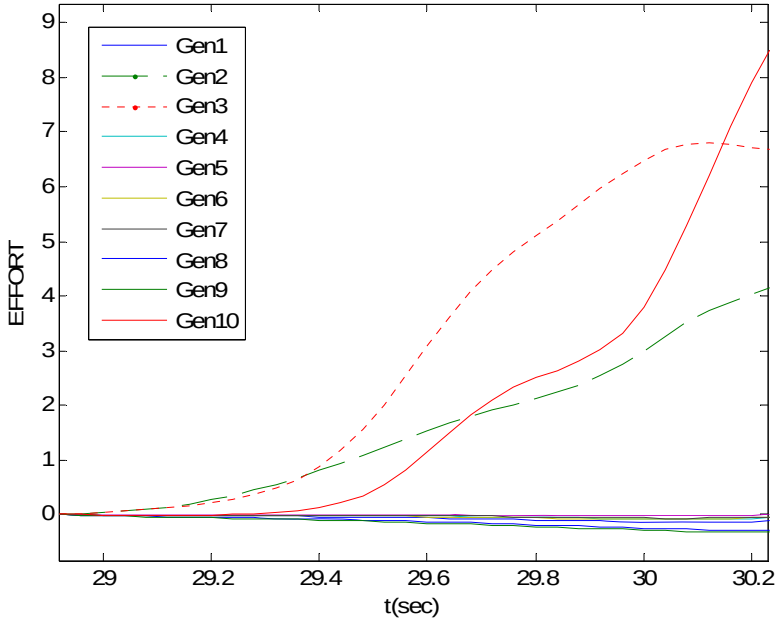

The Effort computed in Figure 5-10 indicates that both Generator 2 and 3 are critical generators thus generation shedding should be initiated at both of them. This agrees with the results from the angle and Lagrangian algorithms.

To make the previous cases stable, it is necessary to shed a significant amount of load. From results on the 39 bus 3-area system it was required to shed at least half the load in that area to regain stability, with regards to the excessive loading cases. The problem with shedding this much load is that voltage levels tend to spike excessively. In

real life applications this can be a serious issue since over voltage protection equipment may cause unnecessary tripping of transformers and lines.

As an example, let us look at the unstable case 2 in Table 5-15. For the control action we shed the same percentage of real power demand as with the reactive power. The control time for the Effort in this case is 26.52 seconds. To make the system stable we need to shed loading at the following busses,

Figure 5- 11: Load Shedding For Contingency 2

	Cont. 2 Load Shed Area 2	
	active (MW)	reactive (MVAR)
bus 39	998.27	209.72
bus 4	546	106
bus 7	244	84
bus 15	344	115
Total	2132.27	514.72
Load Shed %	62.1%	

In this case, it was necessary to disconnect Generators 2 and 3 from the system thus causing a huge deficit in MVAR output in Area 2. To compensate for this it was required that over 2000 MW of load needed to be shed. Looking at the rotor angle in Figure 5-11 we see that Generator 10 stays in synch with the system. The frequency observed in Figure 5-12 indicates that Generator 10 has some damping issues with some large oscillations. The oscillations do damp out however the frequency goes beyond 60.5 Hz. With frequency relays set to operate at 0.2 Hz deviations we see that Generator 10 would have been disconnected from the system leading to a complete isolation of Area 2.

Figure 5- 12: Unstable Cont. 2 Rotor Angle

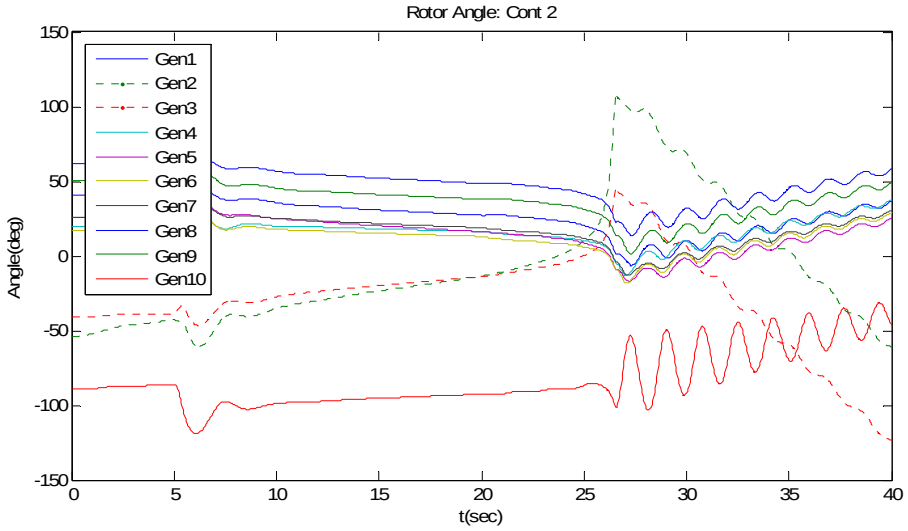

Figure 5- 13: Unstable Cont. 2 Rotor Frequency

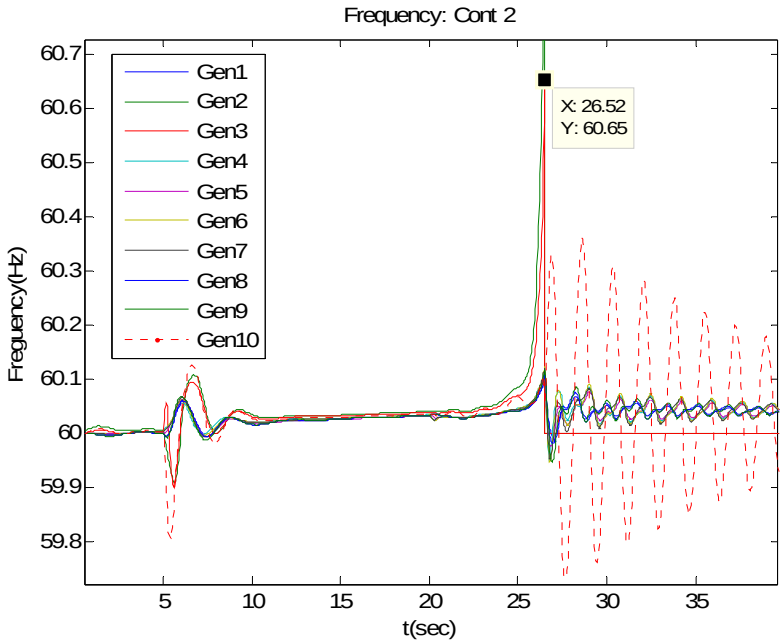

Since we would expect frequency relays to operate sooner then what the control times indicate we could find the energy of each machine are 60.2 Hz and use it as a threshold instead of looking at the maximum stability limit. This of course would make the algorithm more sensitive but we would gain more time in implementing the control action

thus reducing the amount of load shed needed to keep the system synchronized. The other issue is over/under voltage relays. Figure 5-14 shows the voltage magnitude during the transients. At the control time near 26 seconds we see that the voltage spikes to almost 1.2 pu. In some instances this may be enough to trigger voltage relay devices.

Figure 5- 14: Voltage Magnitude, Unstable Cont 2

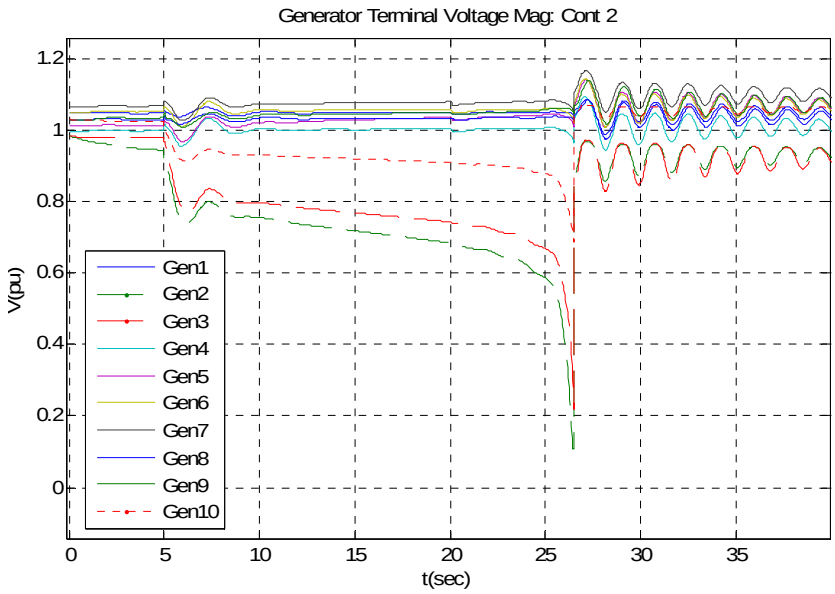

IEEE standards indicate that voltage protection should have a delay of 1s when the spikes are between 1.1 pu and 1.2 pu [15] so for this system we would see some of the relays operate. The following table indicating average voltage protection relay settings was taken from [15],

Table 5- 16: Recommended Voltage Protection Delay Times

Voltage range (% of base voltage[a])	Clearing time(s)[b]
V< 50	0.16
50 ≤ V< 88	2.00
110 < V < 120	1.00
V ≥ 120	0.16

[a]Base voltages are the nominal system voltages stated in ANSI C84.1-1995, Table 1.
[b]DR ≤ 30 kW, maximum clearing times; DR > 30kW, default clearing times.

Table 5-17 [15] tells us that for abnormal frequencies we would also expect Generator 10 to trip since its frequency stays above 60.5 Hz for a greater amount of time than 0.16 seconds. Since Generators 2 and 3 clearly exceed 60.5 Hz as seen in Figure 5-13 they would be disconnected before the control actions could be initiated. Future research is recommended.

Table 5- 17: Frequency Relay Delay Times

DR size	Frequency range (Hz)	Clearing time(s)[a]
≤ 30 kW	> 60.5	0.16
	< 59.3	0.16
> 30 kW	> 60.5	0.16
	< {59.8 – 57.0} (adjustable set point)	Adjustable 0.16 to 300
	< 57.0	0.16

[a]DR ≤ 30 kW, maximum clearing times; DR > 30 kW, default clearing times.

The previous tables were based on connections between transmission systems and distribution level machines. Such an example would be the WSU steam plant. Plants connected through transmission networks in general require tighter tolerances so the values in Tables 5-16 and 5-17 may be under estimated.

5.3 COMMUNICATION DELAY EFFECT

One of the issues of concern in power systems is the time it takes for a measurement to be sent from the PMU to the communication center. Computations are made to determine the control action which also takes time. The control action decided at the communications center is then sent to the corresponding plants where generation shedding/disconnection are required. Using high speed communications the total time delay between the time data is collected and control action initiated is less then 100 ms,

or about 6 cycles. This estimate is made assuming perfect operation, as well as open communication channels at all times. PMU's constitute a new technology so it is difficult to guess how they will be used in the future. So taking into account these issues we simulate the results from the 39 bus 3 Area system using a time delay of 5, 10, and 15 cycles. To judge the effects that the time delay has on the security of the system, we compute the critical clearing time and determine how many cycles it decreases for the given contingency. The impact on algorithm performance is evaluated by comparing the critical clearing time for the base case with the case where delay is added. The critical clearing times for the added communication delays are shown in the Tables 5-18, 5-19, 5-20, and 5-21.

Table 5- 18: Time Delay, Effort Algorithm

	Communication Delay: Effort			
	Critical Clearing Time (Cyc)			
Cont.	No Delay	5 Cyc.	10 Cyc.	15 Cyc.
4 4-14	34.88	34.45	34.16	34.00
5 5-6	25.34	25.20	25.20	25.11
12 12-11	67.26	66.39	65.81	65.33
26 26-29	21.15	19.56	18.12	16.79
29 29-28	20.72	19.85	18.84	17.37
26 26-28	21.29	19.70	18.55	16.99
21 21-22	20.14	19.85	21.73	21.63
23 23-24	20.14	19.99	21.29	21.63
24 24-16	26.04	25.90	25.32	24.84

Table 5- 19: Time Delay, Lagrangian Algorithm

	Communication Delay: Lagrangian			
	Critical Clearing Time (Cyc)			
Cont.	No Delay	5 Cyc.	10 Cyc.	15 Cyc.
4 4-14	40.08	39.79	39.65	39.51
5 5-6	30.25	31.70	29.53	29.24
12 12-11	69.86	69.86	69.86	69.86
26 26-29	20.28	18.84	17.53	16.38
29 29-28	22.01	20.43	18.98	17.54
26 26-28	20.43	18.98	17.68	16.53
21 21-22	20.28	19.85	19.42	19.13
23 23-24	22.31	21.44	20.86	20.43
24 24-16	20.73	20.73	20.87	20.87

Table 5- 20: Time Delay, Angle Algorithm

	Communication Delay: Angle Alg.			
	Critical Clearing Time (Cyc)			
Cont.	No Delay	5 Cyc.	10 Cyc.	15 Cyc.
4 4-14	33.87	33.72	33.58	33.58
5 5-6	25.05	24.91	24.76	24.76
12 12-11	63.93	63.64	63.49	63.35
26 26-29	19.27	18.11	17.10	16.24
29 29-28	17.97	17.39	16.67	15.80
26 26-28	19.42	18.41	17.39	16.38
21 21-22	20.57	19.85	19.27	18.84
23 23-24	20.57	20.00	19.42	18.98
24 24-16	23.31	22.74	22.45	22.02

Table 5- 21: Time Delay, Energy Algorithm

	Communication Delay: Energy			
	Critical Clearing Time (Cyc)			
Cont.	No Delay	5 Cyc.	10 Cyc.	15 Cyc.
4 4-14	33.44	33.44	33.43	33.29
5 5-6	24.76	24.62	25.48	25.48
12 12-11	63.06	63.06	63.06	63.06
26 26-29	19.85	18.41	17.10	15.95
29 29-28	20.00	19.13	17.83	16.53
26 26-28	20.00	18.55	17.25	16.24
21 21-22	17.68	17.83	17.97	17.97
23 23-24	17.97	18.11	18.11	18.26
24 24-16	22.59	22.59	22.59	22.59

The largest decrease in critical clearing times occur at the first five cycles of time delay. At 10 and 15 cycles, the delay effect is less severe for most of the cases. Looking at the previous tables, we see that this change is on average only a few tenths of a cycle. The critical clearing time decreases by about 1 cycle on average for a time delay of 10 cycles. This would suggest that the maximum effectiveness of the algorithms can be achieved if the communications delay is less then 10 cycles. In some of the cases, we can even see an increase in critical clearing time as the time delay increases as is evident in Table 5-21. Since power systems are nonlinear, it is important to consider the state of the system when initiating control action.

CHAPTER 6 CONCLUSIONS

From the simulations on the New England 39 bus system we see that the algorithms are beneficial in maintaining angle stability. With the exception of the individual machine total energy functions, the Angle, Lagrangian, and Effort algorithms were capable of determining the critical generators for both fault and excessive loading cases, most notably the Effort algorithm. Transient disturbances where low voltages lead to angle instability are of more significant importance since local protection of critical lines and transformers fail to operate only rarely, even then there are redundancy schemes to protect against such a case. Under such circumstances it may not be possible to prevent blackouts entirely, but there severity can be reduced. The algorithms presented here show promise in reducing the severity of blackouts.

The use of Effort in determining the real-time status of a disturbed system is a new technique proposed in this thesis. Its use as an indicator of system stability need not be the only use. With more research, it may be possible to implement it into load shedding schemes. Other possible uses may include spin reserve estimation, dynamic security assessment, or generation re-scheduling. Out of the four algorithms presented here, the Effort and Angle algorithms have been shown to be well suited to mitigating angle stability.

The time it takes for data to be measured and be ready for use at control centers is one of the main limitations in real-time implementation. With new advances in communications, it is possible to limit this delay to less then 100 milliseconds. Since power systems are highly nonlinear, no assumption can be made on whether the angle instability gets worse from delays up to 100 ms. Simulations have shown that in some

cases the system is more stable by including the communications delay. Further research is needed.

CHAPTER 7 REFERENCES

[1] "Power System Transient Stability Using Individual Machine Energy Functions," Anthony N. Michel, A.A. Fouad, Vijay Vittal, IEEE Transactions May 1983

[2] "Theory of Nonlinear Control Systems", Nicolai Minorsky, Mcgraw Hill

[3] "Blackout of 2003: Description and Responses", Dennis Ray PSERC, Nov. 5th 2003

[4] "Final Report on the August 14th Blackout in the United States and Canada," U.S.-Canada Power System Outage Task Force

[5] "Power System Transient Stability Analysis Using the Transient Energy Function Method," A.A. Fouad, Vijay Vittal, Prenctice Hall

[6] "Mechanics and Electrodynamics," L.D. Landau, E.M. Lifshitz, Addison-Wesley Publishing 1972

[7] "A Wide-Area Control For Mitigating Angle Instability In Electric Power Systems," Dongchen Hu, MS dissertation, Washington State University, Dec 2006

[8] "Theoritical Concepts In Physics," M.S. Longair, Cambridge University Press 1984

[9] "Adaptive Control of Load Shedding Relays Under Generation Loss Conditions", B. Fox, J.G. Thompson, C.E. Tindall, The Queens University of Belfast IEEE Transactions

[10] "Design of Load Shedding Schemes Against Voltage Instability", C. Moors, D. Lefebvre, T. Van Cutsem, IEEE Transactions 2000

[11] "Automatic Load Shedding in Power Systems", N. Perumal, A. Che Amran, National Power and Energy Conference 2003, Bangi, Malaysia

[12] "An Intelligent Load Shedding (ILS) System Application in a Large Industrial Facility", F. Shokooh, J.J. Dai, S. Shokooh, J. Tastet, H. Castro, T. Khandelwal, G. Donner, IEEE 2005

[13] "Power Generation Operation and Control," Wood, Allen J. Wollenburg, Bruce F., John Wiley and Sons 1996

[14] "Power System Stability and Control" P. Kundur, McGraw-Hill 1994

[15] "IEEE Standard for Interconnecting Distributed Resources with Electric Power Systems", IEEE-SA Standards Board, June 12th 2003

[16] “Synchronized Phasor Data Based Energy Function Analysis of Dominant Power Transfer Paths in Large Power Systems”, Joe H. Chow, Aranya Chakrabortty, Murat Arcak, Bharat Bhargava, and Armando Salazar, IEEE TRANSACTIONS ON POWER SYSTEMS

[17] “E-SIME- A Method for Transient Stability Closed-Loop Emergency Control: Achievements and Prospects”, Mania Pavella, Louis Wehenkel, Daniel Ruiz-Vega, Damien Ernst, Mevludin Glavic, Bulk Power System Dynamics and Control - VII, August 19-24, 2007

[18] “Real-Time Detection of Angle Instability using Synchrophasors and Action Principle”, Michael Sherwood, Dongchen Hu, Vaithianathan “Mani” Venkatasubramanian, Bulk Power System Dynamics and Control-VII, August 19-24, 2007

[19] “WACS-Wide-Area Stability and Voltage Control System: R&D and Online Demonstration”, Carson W. Taylor, Dennis C. Erickson, Kenneth E. Martin, Robert E. Wilson, Vaithianathan Venkatasubramanian, IEEE Procedings, Vol. 93, No. 5, May 2005

CHAPTER 8 APPENDIX

Figure A- 1: 39 Bus 3 Area Test Case

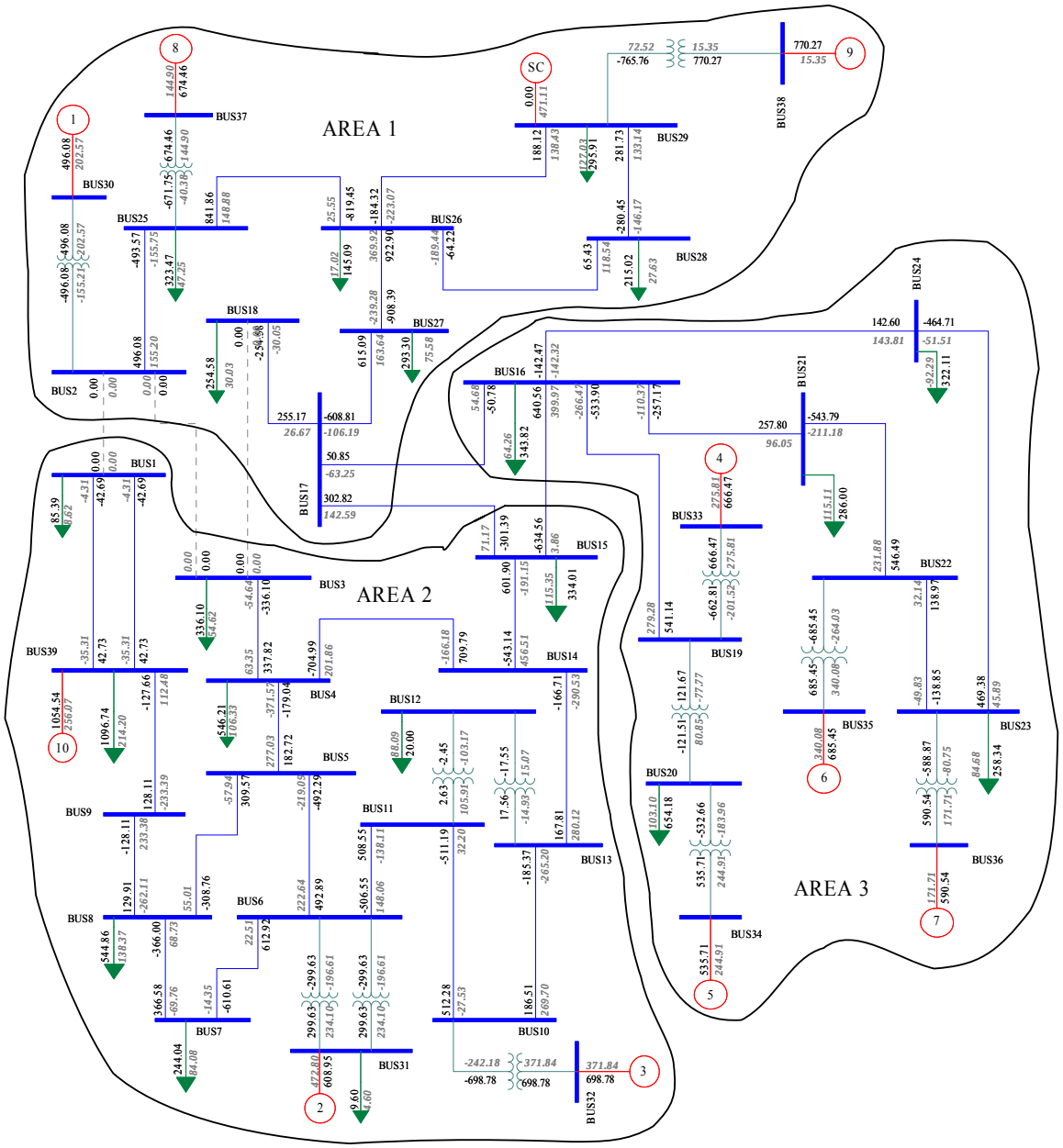

Figure A- 2: Original New England 39 Bus System

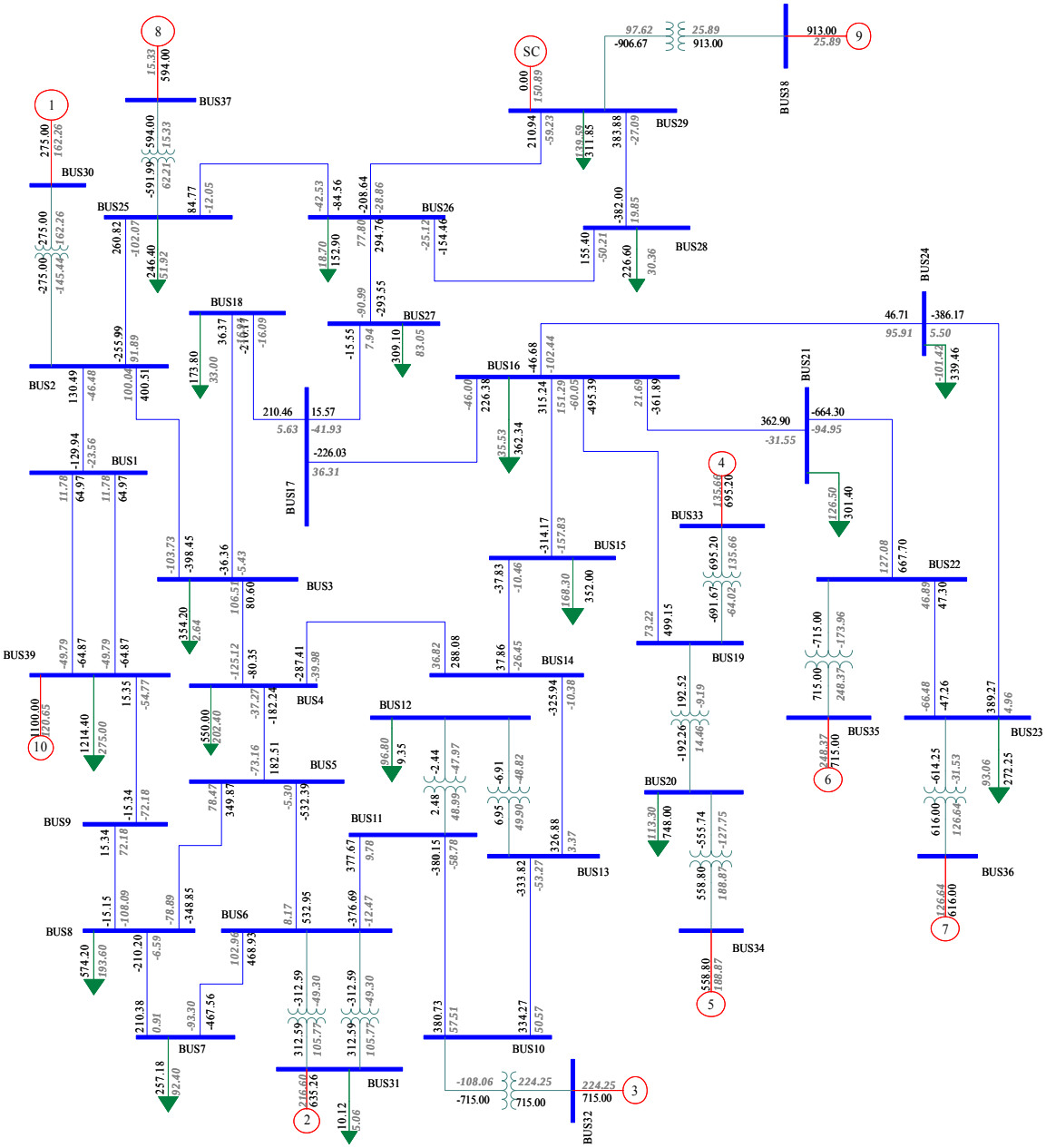

Table A- 1: 39 Bus Overload Contingencies

	39 Bus Overload Contingencies		
	Unstable Contingencies		Stable Contingencies
Cont 1	At Time 5 Seconds	Cont 1	At Time 5 Seconds
	Remove Line 16 to 17		Remove Line 17 to 15
Cont 2	At Time 5 Seconds	Cont 2	At Time 5 Seconds
	Ramp Load bus 4 15%		Ramp Load bus 4 15%
	Change Governor Reference bus 35 40MW		Change Governor Reference bus 35 40MW
	Remove Line 4 to 14		At Time 10 Seconds
	At Time 10 Seconds		Remove Line 10 to 13
	Remove Line 10 to 13		
	Remove Line 7 to 8		
Cont 3	At Time 5 Seconds	Cont 3	At Time 5 Seconds
	Change Governor Reference bus 38 60MW		Change Governor Reference bus 38 60MW
	Ramp Load bus 16 10%		Ramp Load bus 16 10%
	At Time 20 Seconds		At Time 20 Seconds
	Remove Line 15 to 16		Remove Line 17 to 15
Cont 4	At Time 5 Seconds	Cont 4	At Time 5 Seconds
	Change Governor Reference bus 36 40MW		Change Governor Reference bus 36 40MW
	Change Governor Reference bus 34 40MW		Change Governor Reference bus 34 40MW
	Ramp Load bus 15 40%		Ramp Load bus 15 40%
	At Time 15 Seconds		At Time 15 Seconds
	Remove Line 13 to 14		Remove Line 13 to 14
	Remove Line 10 to 13		Remove Line 10 to 13
	At Time 20 Seconds		
	Remove Line 16 to 17		

Table A- 2: Exciter Parameters

39 Bus Exciter Data													
IBUS	KA	TA	VRMAX	VRMIN	KE	TE	KF	TF	E1	SE(E1)	E2	SE(E2)	MVA Base
38	5	0.06	3	-3	1	0.25	0.04	1	3.55	0.08	4.73	0.26	100
37	40	0.02	10.5	-10.5	1	1.4	0.03	1	4.26	0.62	5.68	0.85	100
36	5	0.02	4	-4	1	0.528	0.0854	1.26	3.19	0.072	4.26	0.282	100
35	40	0.02	6.5	-6.5	1	0.73	0.03	1	2.8	0.53	3.74	0.74	100
34	5	0.02	5	-5	1	0.471	0.0754	1.25	3.59	0.064	4.78	0.251	100
33	40	0.02	10	-10	1	0.785	0.03	1	3.93	0.07	5.24	0.91	100
32	5	0.06	3	-3	1	0.5	0.08	1	2.87	0.08	3.82	0.314	100
31	5	0.06	3	-3	1	0.5	0.08	1	2.34	0.13	3.12	0.34	100
30	6.2	0.05	3	-3	0	0.405	0.057	0.5	3.03	0.66	4.05	0.88	100

Table A- 3: 39 Bus Governor Parameters

Governor Parameters									
IBUS	PFL	R	T1	T2	T3	VMIN	Dt	Pgen	Pmax
38	100	0.35	0.1	0	0	0	0	770.3	9999
37	100	0.26	0.1	0	0	0	0	674.5	9999
36	100	0.24	0.1	0	0	0	0	590.5	9999
35	100	0.24	0.1	0	0	0	0	685.5	9999
34	100	0.2	0.1	0	0	0	0	535.7	9999
33	100	0.25	0.1	0	0	0	0	666.5	9999
32	100	0.3	0.1	0	0	0	0	698.8	9999
31	100	0.3	0.1	0	0	0	0	631.1	9999
30	100	0.22	0.1	0	0	0	0	535.1	9999

Table A- 4: Generator 1 to 9 Parameters

Two Axis Model Parameters for Generators 1 to 9													
IBUS	T'do	T''do	T'qo	T''qo	H	D	Ra	Xd	Xq	X'd	X'q	Xl	MVA Base
38	4.79	0	1.96	0	34.5	1	0.0015	0.211	0.205	0.057	0.059	0.03	100
37	6.7	0	0.41	0	24.3	1	0.0015	0.29	0.28	0.057	0.091	0.028	100
36	5.66	0	1.5	0	26.4	1	0.0015	0.295	0.292	0.049	0.186	0.032	100
35	7.3	0	0.4	0	34.8	1	0.0015	0.254	0.241	0.05	0.081	0.022	100
34	5.4	0	0.44	0	26	1	0.0015	0.67	0.62	0.132	0.166	0.054	100
33	5.69	0	1.5	0	28.6	1	0.0015	0.262	0.258	0.044	0.166	0.03	100
32	5.7	0	1.5	0	35.8	1	0.0015	0.25	0.237	0.053	0.088	0.03	100
31	6.56	0	1.5	0	30.3	1	0.0015	0.295	0.282	0.07	0.17	0.035	100
30	5.3	0	1.5	0	20	1	0.0015	0.262	0.258	0.044	0.166	0.03	100

Table A- 5: Generator 10 Classical Model Parameters

Generator 10 Parameters					
IBUS	MVA	Ra	X'd	H	KD
39	100	0	0.02	70	0